

**Powder Metallurgy of Iron-based Matrix Composite with Silicon  
Carbide (SiC) Reinforcement**

by

Siti Nor Fazilah Binti Abdul Basir

Dissertation submitted in partial fulfillment of  
the requirements for the  
Bachelor of Engineering (Hons)  
(Mechanical Engineering)

JULY 2010

Universiti Teknologi PETRONAS  
Bandar Seri Iskandar  
31750 Tronoh  
Perak Darul Ridzuan

CERTIFICATION OF APPROVAL

**Powder Metallurgy of Iron-based Matrix Composite with Silicon  
Carbide (SiC) Reinforcement**

by

Siti Nor Fazilah Binti Abdul Basir

A project dissertation submitted to the  
Mechanical Engineering Programme  
Universiti Teknologi PETRONAS

In partial fulfillment of the requirement for the  
BACHELOR OF ENGINEERING (Hons)  
(MECHANICAL ENGINEERING)

Approved by,

---

(AP. DR. OTHMAN BIN MAMAT)

UNIVERSITI TEKNOLOGI PETRONAS  
TRONOH, PERAK

July 2010

## CERTIFICATION OF ORIGINALITY

This is to certify that I am responsible for the work submitted in this project, that the original work is my own except as specified in the references and acknowledgements, and that the original work contained herein have not been undertaken or done by unspecified sources or persons.

---

(SITI NOR FAZILAH BINTI ABDUL BASIR)

## **ABSTRACT**

Fe-based composites are found to be a promising material for automotive, process and chemical industries but little attention has been given to the study of their properties. This project aimed to study the influences of reinforcement ratios and sintering temperatures on particulate type composite. Pure iron and composite specimens containing 5, 10 and 15 wt.% of SiC particles are fabricated by powder metallurgy technique. The powders are compacted by Auto-Pelletizer equipment at 500MPa and then are sintered in Argon atmosphere for 45 minutes with heating and cooling rates of 5°C/min and 10°C/min, respectively. The obtained Fe-SiC composites are then characterized for density, analysis for microhardness by Vickers Test and microstructural examination using Optical Microscopy. The results show that the hardness of the composites increased with increasing SiC content in accordance with the well dispersed elements observed from optical micrographs. Highest value of hardness; 1634HV is achieved from composite containing 15 wt.% of SiC sintered at 900°C.

## **ACKNOWLEDGEMENT**

Grateful and zillion thanks to Allah s.w.t. for giving health and guidance to finish up this final year project report. First and foremost, I would like to thank my supervisor, Assoc. Prof. Dr. Othman bin Mamat who had taken a lot of efforts in assisting me in conducting this research and his cooperation and endless patience in guiding the me till the completion of the project. Thanks for the advice, plans, and also for the knowledge and experiences shared during my attachment under his supervision.

Besides, I would like to express gratitude to examiners for seminar; AP Dr Faiz Ahmad and AP Dr Patthi Hussin for their comments and advices for the betterment of this project. I would also like to grasp hold of this opportunity to thank various people who indirectly involved in making the project a success; Mr. Irwan, Mr. Faizal, Mr. Sani and all technologists from the Mechanical Engineering laboratories for their kind attention and time to guide and help me to utilize the laboratory equipments. I have very much benefited from their professional experiences and personal advices.

Heartfelt appreciation is given to University Technology PETRONAS (UTP) and Mechanical Engineering Department for equipping me and other students with essential skills and excellent theoretical as well as practical work. To final year project coordinator, I would like to express many thanks for keeping the supervision in great control.

Last but not least, thanks to my beloved parents, family members and all friends for their moral support and valuable contributions throughout the research period. Their encouragement induced excitements to do the very best throughout the semesters.



|   |    |
|---|----|
| <b>REFERENCES</b>   | 41 |
| <b>APPENDIX A - Details of Sintering Conditions</b>                   | 45 |
| <b>APPENDIX B - Figures of Final Samples</b>                          | 47 |
| <b>APPENDIX C - Calculations for Density of Composites.</b>           | 48 |
| <b>APPENDIX D - Table of Dimensions and Green Density of Compacts</b> | 51 |
| <b>APPENDIX E - Table of Sintered Density of Compacts</b>             | 52 |
| <b>APPENDIX F - Table of Hardness (HV) of Compacts</b>                | 53 |

## LIST OF FIGURES

|             |  |    |
|-------------|--|----|
| Figure 2.1  | Plot of hardness versus SiC content for all three models.                              | 9  |
| Figure 3.1  | Flowchart of the methodology   | 17 |
| Figure 4.1  | Green and sintered density versus amount of SiC of compacts sintered at 800°C          | 28 |
| Figure 4.2  | Green and sintered density versus amount of SiC of compacts sintered at 900°C          | 28 |
| Figure 4.3  | Green and sintered density versus amount of SiC of compacts sintered at 1000°C         | 29 |
| Figure 4.4  | Green and sintered density versus amount of SiC of compacts sintered at 1100°C         | 29 |
| Figure 4.5  | Sintered density versus amount of SiC compacts for all sintering temperatures          | 30 |
| Figure 4.6  | Hardness (HV) versus amount of SiC of compacts sintered at 800°C                       | 33 |
| Figure 4.7  | Hardness (HV) versus amount of SiC of compacts sintered at 900°C                       | 33 |
| Figure 4.8  | Hardness (HV) versus amount of SiC of compacts sintered at 1000°C                      | 34 |
| Figure 4.9  | Hardness (HV) versus amount of SiC of compacts sintered at 1100°C                      | 34 |
| Figure 4.10 | Hardness (HV) versus amount of SiC of compacts sintered for all sintering temperatures | 35 |
| Figure 4.11 | Micrograph from optical microscope.  | 38 |

## LIST OF TABLES

|           |  |    |
|-----------|--|----|
| Table 3.1 | Composition of composites based on weight percentage.  | 22 |
| Table 4.1 | Percentage by weight and volume, amount of powders used and theoretical density.                             | 25 |
| Table 4.2 | Result from compaction by Auto Pelletizer  | 26 |
| Table 4.3 | Summary of micro-Vicker Test for all samples   | 32 |
| Table 4.4 | Micrographs from optical microscopy for all compacts with various amounts of SiC and sintering temperatures. | 37 |

# CHAPTER 1

## INTRODUCTION

### 1.1 Project Background

#### 1.1.1 Characteristics of Metal Matrix Composites

Metal matrix composites (MMCs) are widely used in components of various pieces of industrial equipment. The purpose of producing a composite material is to achieve an enhanced combination of properties by combining at least two different material phases with dissimilar properties. Compositing makes it possible to create materials with properties unattainable in typical monolithic materials. MMCs generally combine the properties of metal matrix which are the ductility and toughness, with a high thermal strength reinforcing material; the ceramic. MMCs have been given an increasing amount of attention and application in recent years due to developments in processing methods and the increasing understanding of structure-property relationships (Franklin, 2003).

Basically, MMCs are characterized by the type of reinforcement used. Commonly used composite types include continuous fibers, short fibers, whiskers, particulate, and flakes. The reinforcement types can be further divided into two categories; continuous and discontinuous form. Franklin (2003) describes that the continuous fiber reinforced composite has excellent axial strength for uniaxial load application, but there are disadvantages associated with the fabrication including fiber damage and microstructural non-uniformity (Ibrahim et.al, 1991). Short fibers, whiskers and particulates fall under the group of discontinuous reinforcement. Properties of the composite are affected by the

size, aspect ratio, and volume fraction of the reinforcement. There are many advantages of using discontinuous reinforcement over the continuous type especially in the transverse properties and cost of fabrication.

A variety of processes have been and are being developed for the fabrication of MMCs including spray forming, vapor deposition, casting, powder metallurgy, hot press and interleave or diffusion bond. Each technique has its own limitations in term of component size and shape, and imposed certain microstructural features on the product. The most broadly used method to manufacture MMCs is the powder metallurgy (PM) technique. PM is an excellent method because it offers a means of adding possibly high volume percentage of hard reinforcing phases in a uniform distribution compared to casting or spray forming technique.

### **1.1.2 Development of Powder Metallurgy Technique**

Powder metallurgy components are increasingly replacing wrought materials in high performance applications. According to Smith (2003), the first known application of powder metallurgy technology, around 3000 BC, involved production of iron tools in ancient Egypt using a procedure that involved heating iron oxide and hammering the resulting sponge iron to the required shape. Evidence has been found for the existence of similar techniques in other parts of the ancient world including the discovery of the most impressive development of the efforts in Delhi Pillar, which weighs nearly six tonnes. Following the practice, there was a long period without progress until the eighteenth century that activities in Europe signified the initiation of modern PM technology with the manufacturing of platinum-arsenic alloy for building chemical vessels.

Generally, PM technique is utilized in the fabrication of metallic materials but the principle of the process apply with little modification to ceramics, polymers and a variety of composite materials composed of metallic and non-metallic phases. During the past decade there have been significant advances in PM

technology. New types of powders especially in the form of rare composites with superior properties are introduced, allowing the production of larger and higher strength materials. Difficult to process materials, where fully dense high performance alloys can now be processed with uniform microstructure, and multiphase composite with a wide combination of properties can be economically synthesized with the advancement of PM technique.

Production of metal matrix composites through powder metallurgy technique is not new to the industry. The focus of the selection of suitable process for fabrication of MMCs is the desired kind, quantity, and the distribution of the reinforcement components, the matrix alloy and the application. For MMCs, PM is costly but is suitable for small components. Plus, PM offers unlimited addition of volume of reinforcement and matrices in the process. Of the PM research that has been completed, most relates to materials behavior and effects of various parameters concurrent with PM technique. Many of the researches are in any case worthy of study, since it has resulted in numerous interesting and useful findings for improving each single process involves in PM method.

## **1.2 Problem Statement**

In recent years, the development of metal matrix composite (MMCs) has been receiving worldwide attention on account of their superior strength and stiffness in addition to high wear resistance and creep resistance comparison to their corresponding wrought alloys. In line with this, powder metallurgy process and technology appears to build up a wide array of concern among researchers. A large number of research papers published focuses on the application of powder metallurgy towards light metal matrix such as Al, Ti and Mg. The cost of processing these materials is a significant constraint on continued growth of the market.

It is also found that there are rare report on other metal matrix composites, especially Fe-based which is found to be limited. Although this composite are promising materials for the process industries, little attention has been given to the study of their properties. Fe is used in great quantities in the automotive industries as well as in ferromagnetism. Thus, it is an interesting idea to conduct a research to verify the suitability and introduce the Fe-based composite with hard particle reinforcement by application of powder metallurgy technique, which is the most appealing fabrication process for MMCs.

## **1.3 Objective and Scope of Study**

Main objective of this project is directed towards the study on producing Fe-based composite using powder metallurgy technique. The study aims to introduce Fe as a possible metal matrix to be reinforced with SiC ceramic particle and to determine the effect of particulate SiC content towards the hardness of Fe-SiC composite. This study employs a complete powder metallurgy process cycle, including the powder production, mixing, compacting, and sintering. For this study, the scopes are restricted to ceramic particulate reinforced Fe metal matrix systems, with variation of the composites ratio and sintering temperatures. Final products will be examined by outlining the mechanical properties, focusing on the hardness and characterizing the microstructure by observation with Scanning Electron Microscopic (SEM) or Optical Microscopy (OM). The works will be carried out in the period of two semesters in 2010.

## **CHAPTER 2**

### **LITERATURE REVIEW**

#### **2.1 Introduction**

Literature survey is carried out to have an overview of the production process, properties, and mechanical behavior of metal matrix composites (MMCs). A large number of papers concerning the employment of powder metallurgy technique to fabricate MMCs have been published. According to Zebarjad et al. (2008), the papers concentrated on MMCs can be categorized into some major groups as elaborated further in later paragraphs.

The studies of the first group focused on manufacturing methods. The results of their studies showed that there are some different techniques for fabrication of MMCs. The methods are squeeze casting, metal spray, metal infiltration, laser deposition technology and mechanical milling, powder technology, and so on. Among them, powder metallurgy presents one of the biggest advantages, although there are a lot of problems concerning the distribution of the reinforcement in the composite matrix. The second group tried to investigate the role of reinforcement particles on formability of metal matrix. Their result show that the particles play like a barrier against metal flow.

Next, the third group of researches worked on corrosion behavior of MMCs. They demonstrated that the weight loss of the composites in corrosive media depends strongly on both volume percent and particle size of reinforcement. The studies of another group concentrated on the role of reinforcement particles on mechanical properties and machinability of MMCs. They showed that both volume percent and particle size of reinforcement particles play an important role on mechanical behavior of MMCs. Finally, the last investigations concentrated on the mechanical, optical, thermal,

and electrical properties of the composite. The results illustrated that the mentioned properties vary as volume percent and particle size of reinforcement change.

Apart from this, other related papers will also be discussed in this section. Since, powder metallurgy products are typically produced in sequence of powder production, cold compaction, and sintering operation, the best parameters of each step will be reviewed based on successful researches. Results from the studies are taken as the main reference for designing the methodology for present investigation.

## **2.2 Material Aspects**

Metal matrix composites materials have a combination of superior properties compared to unreinforced matrix which are; improved wear resistance, higher elastic modulus, higher service temperature, increased strength, high thermal and electrical conductivity, low coefficient of thermal expansion and high vacuum environmental resistance. Properties of composites are strongly influenced by the properties of their constituent materials. The superior properties can be attained with the proper choice of matrix and reinforcement.

### **2.2.1 Matrix Material – Why Fe?**

The main function of matrix in MMCs is to transfer and distribute the load to the reinforcement. This transfer of load depends on the bonding which depends on the type of matrix and reinforcement and the fabrication technique. Generally Al, Ti, Mg, Ni, Cu, Pb, Fe, Ag, Zn, Sn and Si are used as the matrix material, but Al, Ti, Mg are used widely. But those widely used matrix are relatively expensive in both the material cost and in term of fabrication.

Pagounis et al. (1996) stated that, Fe (iron) matrix composites are a new class of advanced materials proposed mainly as inexpensive wear-resistant parts. It is interesting to use iron and its alloys as the matrix material in composite systems because of their low cost, the possibility of heat treatment and technological

effectiveness. In the other hand, iron based composites show higher hardness, higher compressive strength, and the elastic modulus is the highest for machinable and hardenable materials.

The statements are seconded by Tanino et al. (2008), which claim that sintered iron-based materials has good wear resistant, improved strength and machinability properties. However, compared with their unreinforced alloys, iron matrix composites suffer from lower ductility and toughness. Though, reductions in yield and ultimate tensile strength which revamp the weaknesses through the addition of hard particle reinforcement have also been reported by several researches including: Mukherjee et al (1985), Bryggman et al. (1992), and Talvite et al. (1994).

### **2.2.2 Reinforcing Material – Why SiC?**

Composites consist of one or more discontinuous phases embedded in a continuous phase (the matrix). The discontinuous phase which is usually harder and stronger than the continuous phase is called the reinforcement or reinforcing material. As stated by Prasad (2006) in his thesis on the development and characterization of metal matrix composite;

For metal reinforcement, ceramics particle or rather, fibers or carbon fibers are often used. Reinforcement increases the strength, stiffness and the temperature resistance capacity and lowers the density of MMCs. In order to achieve these properties the selection depends on the type of reinforcement, its method of production and chemical compatibility with the matrix, sizes, shapes, surface morphology, structural defects, impurities and inherent properties. (p.24)

As per quoted above, two main types of reinforcing materials that are widely used that are the particles and fibers. Both types of reinforcement produce reinforcing effects in metallic matrices by different strengthening mechanisms. Focus is given to the ceramic particulate type of reinforcement since it is said by Prasad (2006) as the most suitable material to be mixed with metal matrices.

Ceramic particles which have been proposed for use as reinforcements in iron-based composites include carbides (TiC, WC, VC and SiC), oxides ( $\text{Al}_2\text{O}_3$ ,  $\text{ZrO}_2$ , and  $\text{Y}_2\text{O}_3$ ), nitrides (TiN and  $\text{Si}_3\text{N}_4$ ) and borides ( $\text{TiB}_2$  and  $\text{CrB}_2$ ). Zhang et al. (1992), verify from their research on “Damping Characteristics of Graphite Particulate Reinforced Aluminium Composites” that the use of graphite reinforcement in a metal matrix has a potential to create a material with a high thermal conductivity, excellent mechanical properties and attractive damping behavior at elevated temperatures.

In addition to that, research conducted by Chakthin et al. (2008) on Fe-based composites reinforced with WC and SiC particles respectively, proves that SiC is a better reinforcing material. Their investigation rigidly reveals that the strengthening effect and phase transformation did not exist in Fe-WC compared to Fe-SiC composite.

### **2.2.3 Particle Size and Volume Fraction**

Chawla et al. (2001), claimed that in metal matrix composites, particle reinforced materials are more attractive due to their cost-effectiveness, isotropic properties, and their ability to be processed using similar monolithic materials technique. It is supported by Prasad (2006) which stated that the strength of particle-reinforced composites is observed to be most strongly dependent on the volume fraction and particle size of the reinforcement. For that reason, most of the MMCs introduced are in the initial form of metal matrix powder embedded with particulate reinforcement. Properties of this type of composites are affected by the size, aspect ratio, and volume fraction of the reinforcement.

Since research concerning Fe-SiC composites is off-focused, the literatures on effect of particle sizes and volume fractions of the material are limited. In research conducted by Chakthin et al. (2008) about the influence of carbides on properties of sintered Fe-based composites, they found that for sintered Fe-SiC composites, tensile strengths and hardness, superior to those of the sintered Fe material,

increased with decreasing carbide particle size. To further discuss this factor, literatures on other metal-based composites which are significant to the findings are referred.

Lin et al. (2003) conducted a study about the effect of reinforcement particles on the strengthening mechanism for Cu-SiC composite. In the research, they designed three models containing different sizes of reinforcing particles:

- Model I: The size of the reinforcing particles is approximately the size of the matrix particles.
- Model II: The ratio of the reinforced particle size to the matrix particle size exceeds 2.
- Model III: The reinforcing particles are much smaller than the matrix particles.

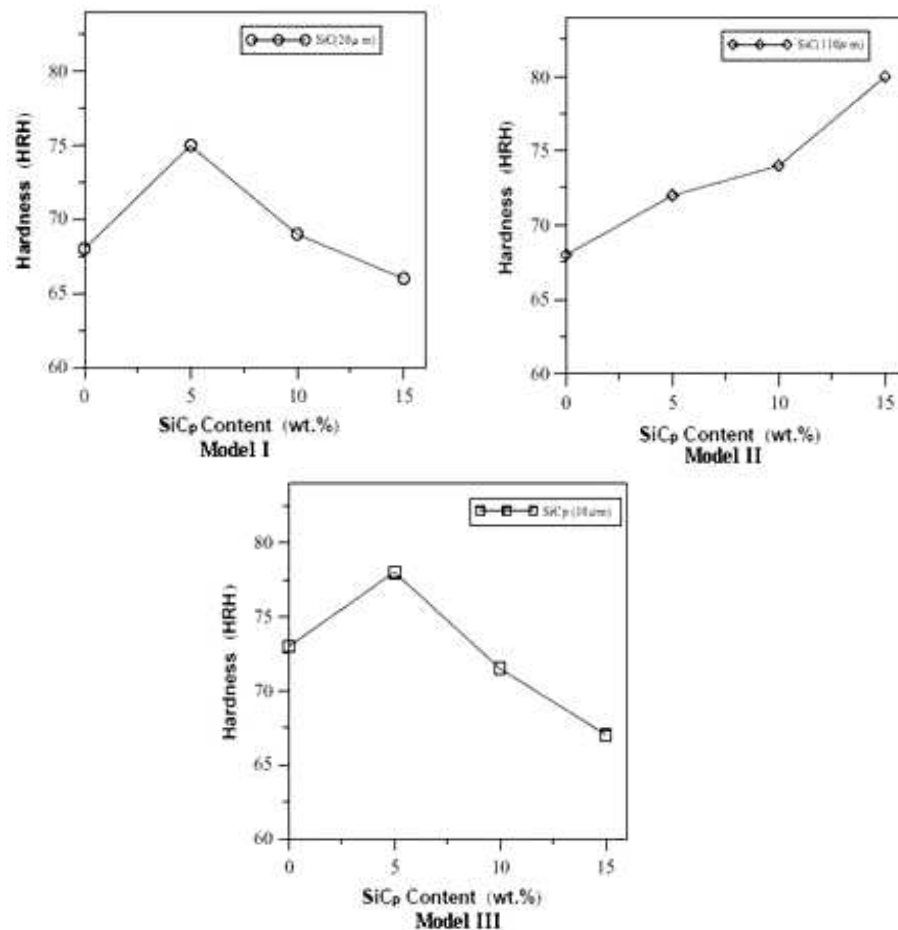


Figure 2.1: Hardness versus SiC content for all three models.

Results as show in Figure 2.1, demonstrate that all three models can produce an effective strengthening mechanism with additional variable; the volume fraction. For Model I and III, they discovered that there is an optimum value of SiC content, approximately 5% of volume fraction to obtain the optimum hardness. Whereas, the hardness of the composite increases with the increasing of SiC content in Model II. This is because; SiC particles can effectively obstruct boundary slippage between the interfaces of Cu particles and impede the plastic flow to hamper any deformation. All in all, in term of size of reinforcement particle, Model III which contains reinforcing particles that is much smaller than the matrix particles produced highest value of hardness at the same volume of SiC.

Chawla et al. (2001), proposed that, “an increase in reinforcement volume fraction or decrease in particle size increase the amount of indirect strengthening, since a larger amount of interfacial area exists for dislocation punching to takes place” (p.357). It is said that the difference in strengthening between unreinforced and composite could be attributed primarily to load transfer to the reinforcement. Thus, with increasing volume fraction, more loads are transferred to the reinforcement, which resulted in higher strength of the composite.

In addition to that, the findings are in line with theory of the effect of particle sizes and research by other authors. According to Yu et al. (2007), statistically, larger flaws and more defects are more likely to exist in larger particles and, therefore, will deteriorate the strength of composites when compared with the composites containing smaller particles. This is likely due to the smaller particles of reinforcement can be inserted into the voids among the matrix particles easily, increasing the density and bonding strength of MMCs. Additionally, smaller particles will exert more constraint on grain growth which can also contribute to the increase of strength. Relationship of the particle size on the mechanical properties of MMCs is graphically proposed by Zhang et al. (2004) as a result of his study which is to illustrate the relationship between reinforcement particle size ( $R$ ) and mechanical properties (e.g. yield strength,  $\sigma_y$ ).

The research claims that, the strengthening effect increases with increase of particle size of very fine and shearable inter-metallic precipitates. However, these precipitates are not stable at high temperatures, and once the particle size is higher than a certain value, they become non-shearable or “hard” particles, and the strengthening effect becomes weaker with increasing particle size. In the meantime, smaller particles are less prone to having internal defects and thus are more difficult to be fractured. These factors are favorable for achieving high strength and good fracture toughness. In addition, the ceramic particles are stable at high temperatures, so the strengthening effect will hold at high temperatures, leading to a high creep resistance when creep is dislocation controlled.

### **2.3 Powder Metallurgy Processes**

Apart from casting, melt infiltration, and spray-formed method, powder metallurgy (PM) technique is the one of the most commonly used process for the fabrication of discontinuous reinforced MMCs. PM technology appears to build up a wide array of concern among researchers. PM is costly, but suitable for small components. Prasad (2006) chronologically simplifies the methodology of PM process as quoted below.

In general process, the powders of matrix materials and reinforcement are first blended and fed into a mould of the desired shape. Pressure is then applied to further compact the powder (cold pressing). In order to facilitate the bonding between the powder particles, the compact is then heated to a temperature that is below the melting point but sufficiently high to develop significant solid-state diffusion (sintering). The consolidated product is then used as a MMC material after some secondary operation. (p.30)

In summary, 3 main steps of PM are mixing, compaction and sintering. Since pressing (compaction) and sintering have the most significant effects towards the mechanical properties of MMCs, detail literatures on both processes will be discussed further in this section.

### **2.3.1 Powder Compaction**

Conventional PM technique uses cold compaction method to press the powder into green compact. Kim et al. (2000) claimed that non-uniformity density distribution of powder compacts under cold compaction has a great influence on the subsequent process such as sintering. The early attempts on research regarding compaction focused on densification and concentrated on the variation of either axial or radial stress with compact sectional area, height, surface area, and friction coefficient (Smith, 2003). Compaction as describe by Kalpakjian et al. (2006), are meant to obtain required shape, density and particle to particle contact and to make the part sufficiently strong for further processing. There are several types of cold compaction method utilizes in PM, namely cold isostatic pressing and cold die compaction.

Research conducted by Kim et al. (2000) on the cold compaction of composite powders, experimented the densification behavior of mixed copper and tungsten powders under cold isostatic pressing and die compaction. Copper powder is regard as the soft metals whereas tungsten powder is the opposite. To correlate the case on composite, tungsten powder can be regarded as the hard particle, or ceramics. It is observed that, in the cold isostatic pressing, as pressure increases, copper powder deform markedly, but tungsten powder do not deform as much. Also, more pores are observed in composite powder compacts as the volume fraction increases. From microstructural view, it is found that the powder compacted by cold die compaction is less homogeneous than that by cold isostatic pressing because of deviatoric stress.

Generally, density of the green compact depends on the pressure applied. As the compacting pressure increase, the powders become denser due to the decreasing of free space in between the particles. Kalpakjian et al. (2006) outlined the size distribution of the particles as an important factor in compaction-density relationship. They stated that;

If all of the particles are of the same size, there always will be some porosity when they are packed together, theoretically a porosity of at least 24% by volume. Introducing smaller powder into the powder mix will fill the spaces between the larger particles and thus, result in a higher density of the compact. (p.491)

From the statement, it is likely to conclude that the density of compacted powders also depends on powder sizes apart from its dependency on the compaction pressure applied. The suitable compacting pressure for Fe-based material as proposed by the same authors range between 350-800MPa and so far, research regarding the optimum pressure for Fe-based composite are yet to be found.

Other than density, issues related to compaction phase includes; the sizes of particles and mechanism of deformation which holds major effects towards the strengthening behavior. As stated by Lin et al. (2003), there are two modes of deformation under compressive stress which are the grain deformation and boundary slip. When the size of the reinforcing particles is approximately the size of the matrix particles, boundary slips causes plastic deformation when stress is applied. Whereas, then the ratio of reinforcement particle size to the matrix exceeds two, the reinforcement particle will effectively obstruct boundary slippage at the interfaces between matrix which cause grain deformation to take place. Their study reveals that mechanism of plastic causes by grain deformation are preferable than boundary slips to produce an effective strengthening by reinforcement.

### **2.3.2 Sintering**

Sintering is one of the most important processes in PM and plays the crucial role in the properties and cost of final products. Kalpakjian (2006) define sintering as “the process whereby green compacts are heated in a controlled atmosphere furnace to a temperature below the melting point but sufficiently high to allow bonding by fusion of the individual particles”. Sintering plays a major role in improving the density of the raw material by means of reducing porosity. It is said that, the changes in pore structure depend on many details, including the initial pore size

distribution and sintering conditions. Most of the established study on sintering mechanisms centered on the stages of sintering, effects of sintering time and temperature, and influence of additives and phases.

Fe-SiC composites produced in the experiment conducted by Chakthin et al. (2008) exhibit an increasing in hardness with the increasing of sintering temperature. It is said that the stability of carbide particles under sintering conditions is the prime factor controlling properties of the sintered Fe-carbide composites. As per their study, it is observed that some of SiC particles decomposed into Si and C atoms that could diffuse into the Fe particles which resulted in growth of voids surrounding SiC particle as well as decreasing the particle size.

Besides, Tanino et al. (2008) who patented a research entitled “Iron-based sintered material and production method thereof” claims that

When the heating temperature is lower than 1100°C, it is not possible to sinter the powder sufficiently and thus not possible to improve the quenching efficiency of the sintering material. It is not possible to improve the fatigue strength and machinability, when the heating temperature is higher than 1170°C, and it is not possible to improve one or both of the fatigue strength and machinability, when the heating period is shorter than 10 minutes or longer than 30 minutes.

A portion of the claims is agreed by Feng et al. (2007) when they conducted experiment on intensified sintering of iron powders under the action of an electric field. The result shows that the density of sintered compacts is lower for sample from 1350°C compared to samples from 1100°C where an optimum sintered density is obtained. This can be theoretically explained with the principle of sintering kinetics which stated; the higher the sintering temperature, the higher densification degree, but too high temperature is unfavorable for the densification process (Mrowee, 1980). This is due to the process of pore expansion or Ostwald ripening that occurs at high sintering temperature because of the effect of plastic deformation.

## 2.4 Mechanical Properties and Microstructure

Focusing on strengthening effect for the present study, Chawla et al. (2001) described in detail about the behavior of particulate MMCs. The difference in strengthening between the unreinforced material and composites could be attributed primarily to load transfer to the reinforcement as further quoted below.

Under an applied load, the load is transferred from the weaker matrix, across the matrix/reinforcement interface, to the typically higher stiffness reinforcement. In this manner, strengthening takes place by the reinforcement “carrying” much of the applied load. Due to the lower aspect ratio of particulate materials, load transfer is not as efficient as in the case of continuous fiber reinforcement, but still significant in providing strengthening. (p.357)

Apart from the properties discussed respectively with the contributing factors above, according to Prasad (2006), it is apparent that parameters controlling the mechanical properties of particulate reinforced composites are still not understood in any convincing details. Nevertheless, some of the important factors have been highlighted from literatures.

- The strength of particle reinforced composites is observed to be most strongly dependent on the volume fraction of particle and size of the reinforcement.
- Dislocation strengthening will play a more significant role in MMCs than in the unreinforced alloy due to the increased dislocation density.
- Greatest concern appears to be on the introduction of defects and inhomogeneities in the various processing stages, which has been found to result in considerable scatter in mechanical properties.

Besides, the microstructural features of the fabricated composite can also assist in interpreting the mechanical behavior of the MMCs especially by observation of the distribution of materials. It is claimed by several investigators that the properties of composites are finally dependent on the distribution of the particles in the composite. The distribution of particles depends on the processing and fabrication routes involved.

Results obtained from Chakthin et al. (2008) revealed that there existed three different microstructural features in sintered Fe-SiC composites, apart from the non-melted SiC. It is due to the decomposition of SiC particles and the existence of different iron phases namely pearlite and austenite. The formation of iron-carbon phases directly contributed to an effective strengthening mechanism in the composite.

# CHAPTER 3

## METHODOLOGY

In order to conduct the research project, the flow of methodology is designed as follow:

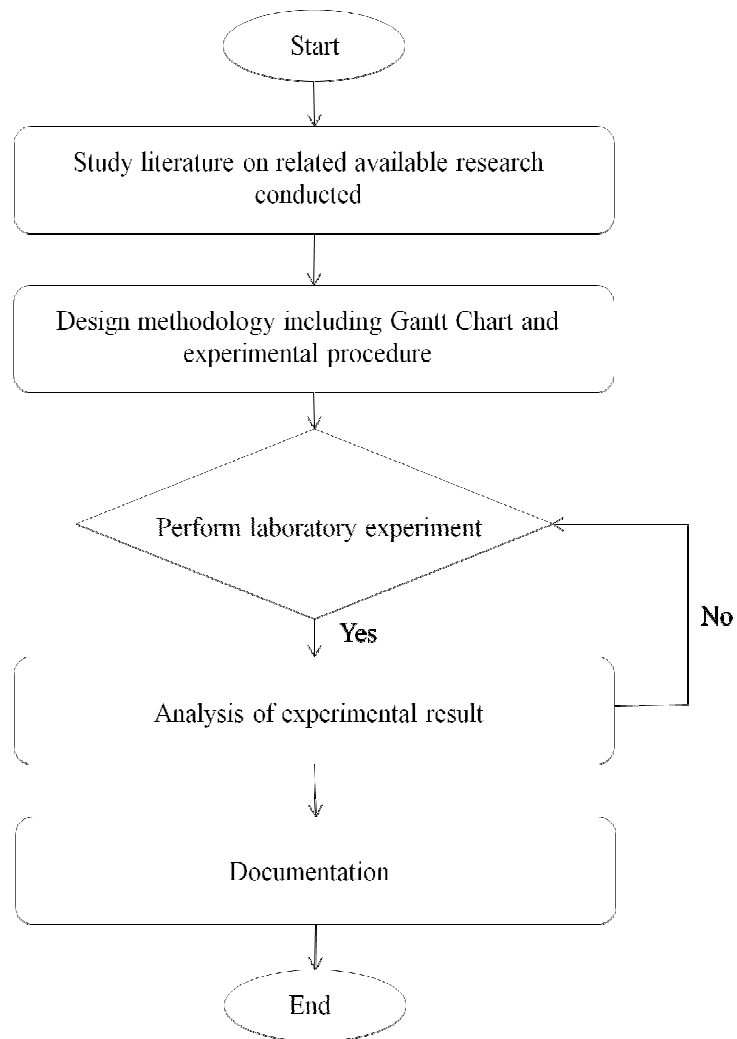
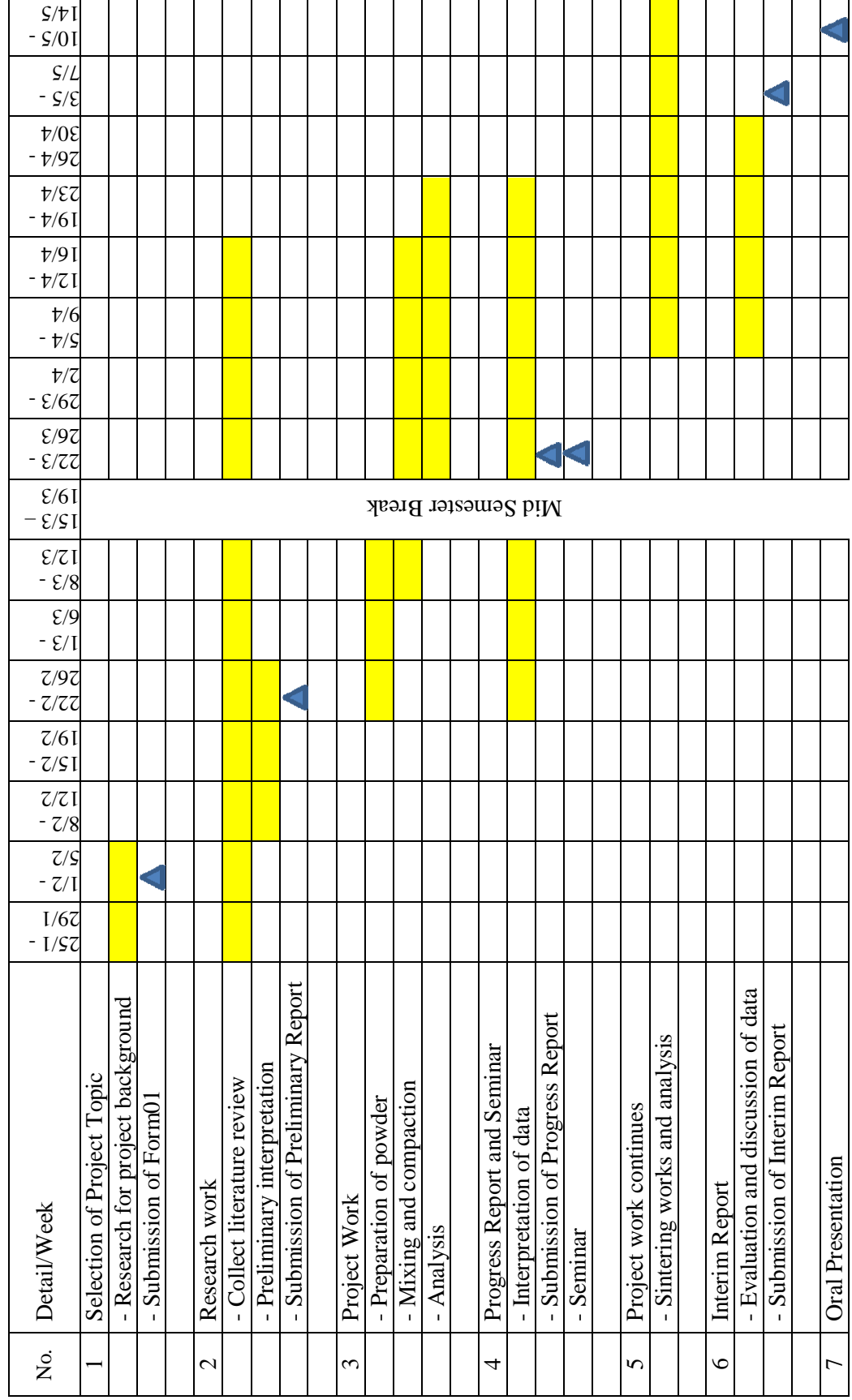


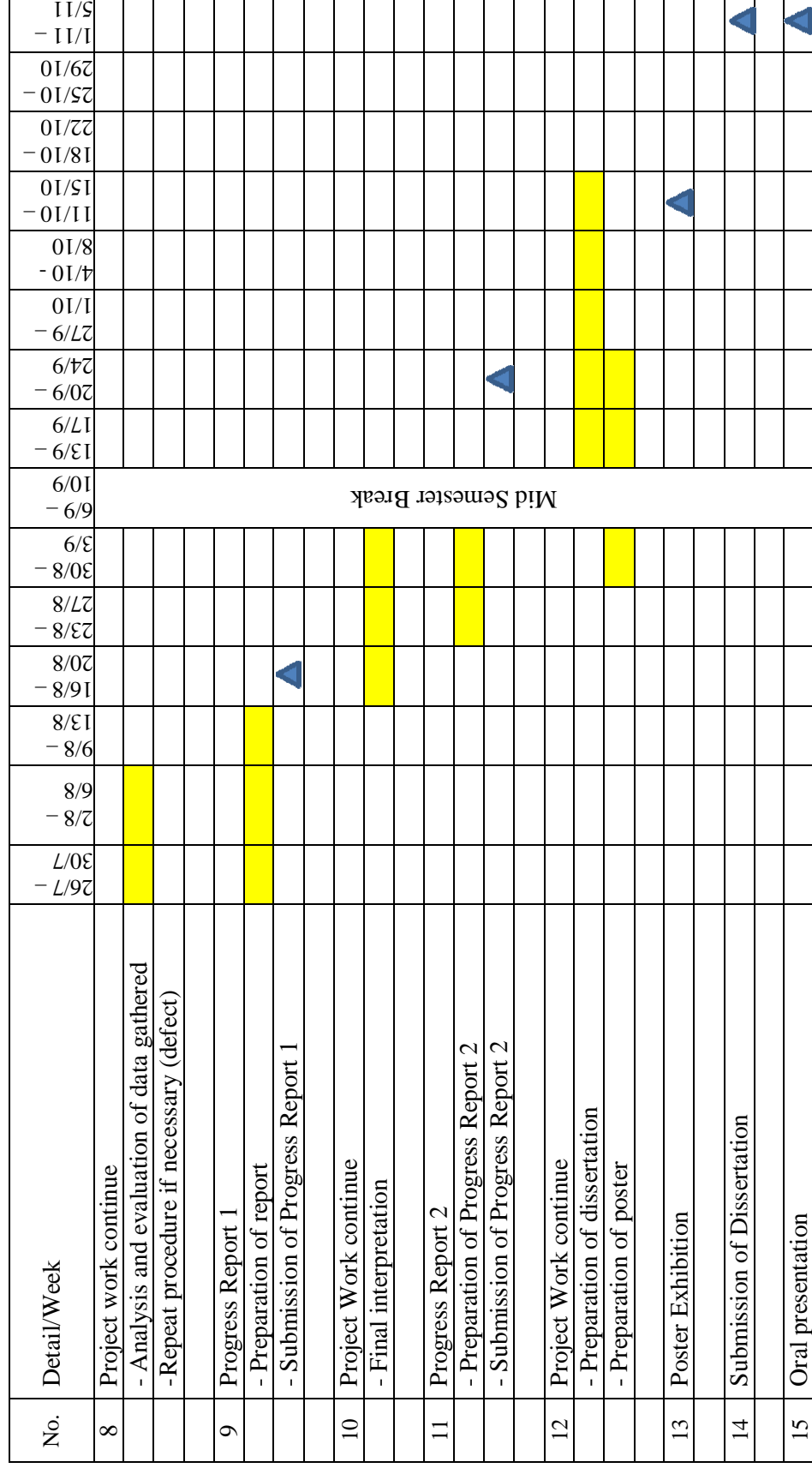
Figure 3.1: Flowchart of the methodology.

Throughout the stages of research, the listed steps shown in the flowchart in Figure 3.1 were followed accordingly. Details of the flow are described in Gantt chart shown in the following section.

### 3.1 Gantt Chart of the project



### 3.1 Gantt Chart (continue)



 Key milestone

 Process

 Process

## **3.2 Laboratory Works**

### **3.2.1 Materials**

A number of 48 samples of SiC reinforced Fe composite with 0%, 5%, 10%, and 15% weight percentage are required for the experiment. Raw materials needed to produce the samples are 89g of iron powder as the metallic matrix and 8g of Silicon Carbide (SiC) powder for the ceramic reinforcement.

### **3.2.2 Tools and Equipments**

The following are major tools and equipments that are used in the laboratory experiment for the research:

- i. Weighing scale
- ii. Marble mortar and pestle
- iii. Auto Pelletizer
- iv. Archimedes density measuring equipment
- v. Sintering furnace
- vi. Hot mounting machine
- vii. Grinder and polisher
- viii. Sand papers
- ix. Scanning Electron Microscopic (SEM) tool
- x. Hardness Tester (Vickers)

### **3.2.3 Experimental procedure**

- i. 89g of Fe powder and 8g of SiC powder are prepared.
- ii. The characteristics of the powders including the particle sizes, and density are recorded.
- iii. The weighing scale is calibrated to ensure accuracy.
- iv. The amounts of powders as tabulated in the following page are weighted carefully.

Table 3.1: Composition of composites based on weight percentage.

| Powder No. | Quantity | Fe  |            | SiC |            |
|------------|----------|-----|------------|-----|------------|
|            |          | %   | Weight (g) | %   | Weight (g) |
| 1          | 12       | 100 | 2.00       | 0   | 0.00       |
| 2          | 12       | 95  | 1.90       | 5   | 0.10       |
| 3          | 12       | 90  | 1.80       | 10  | 0.20       |
| 4          | 12       | 85  | 1.70       | 15  | 0.30       |

- v. The powders are mixed using marble mortar and pestle to form a homogeneous mixture.
- vi. Using auto-pelletizer, the powders are compacted at approximately 500MPa with dwell time of 5 minutes.
- vii. The compact is removed from die.
- viii. The compact is weighted, its dimension is recorded and the green density is determined.
- ix. The steps are repeated to produce the rest of the samples.
- x. Using a sintering furnace, 3 compacts of each composition are sintered at temperatures starting from 800°C, 900°C, 1000°C, and 1100°C for 45 minutes. The heating and cooling rates of the sintering process are 5°C/minute and 10°C/minute respectively. (Plots of the sintering conditions are attached in Appendix A)
- xi. The sintered compacts are weighted, their final dimensions are recorded, and their sintered densities are determined using Archimedes density measuring equipment.

#### 3.2.4 Polished specimen preparation

The composite compacts were mounted using hot mounting machine. The mounting media used is Phenolic powder which was poured into the mounting press according to desirable mounting height. The process involved heating Phenolic powder above 150°C at a constant pressure about 30Mpa for a cycle time of 15 minutes. The mounted compacts are then cleaved off using the

Polisher and Grinder machine. Three grades of sand papers (260, 600, and 1200 grit) are used to polish the compacts at 150 revs speed of the grinder plate. Pictures of the polished samples are attached in Appendix B.

### **3.2.5 Analysis procedure**

Analysis of samples includes performing hardness test by applying Vickers Hardness Tester and characterization of microstructure using Scanning Electron Microscopy (SEM) tool. For the hardness test, the surface of a pallet were subjected to a pressure at load of 300 g with 15s dwell time by means of a pyramid-shaped diamond. The resulting indentation then was measured under a microscope and the Vickers Hardness value read from a conversion table available at the laboratory. After that, the microscopic analysis was performed with assistance from laboratory technologist after completing the preparation and submission of samples. The SEM micrographs were then available for further review. However, due to low quality of images, optical microscopy (OM) were used instead of SEM. Referring to literature (Chakthin et al.2008), OM is also applicable to analyze microstructure of Fe-based materials.

## CHAPTER 4

### RESULTS AND DISCUSSION

Project works was strictly executed based on Gantt chart and have yield reasonable results. Completed steps with initial and final results will be discussed chronologically in this chapter.

#### 4.1 Powder preparation

Powders available at the laboratory are iron (Fe) 10 $\mu$ m and 850 $\mu$ m in size with density of 7.86g/cm<sup>3</sup> and SiC 32 $\mu$ m to 75 $\mu$ m in size with density of 3.22g/cm<sup>3</sup> respectively. Due to some constraint present at compaction stage that will be discussed later, Fe powder of 10 $\mu$ m in size is chosen for the research. From here, it is realized that the size of the reinforcement particles are larger than the size of matrix metal. This current condition is rarely investigated by researchers especially for the Fe-SiC composite case. Thus, the closest reference apart from paper by Chakthin et al. (2008) which specifically describe Fe-SiC composite is the research conducted by Lin et. al (2003) on the strengthening mechanism in Cu-SiC composite with variations in particle sizes.

In their research, under the same condition of particle sizes, it is observed that the smaller matrix particle will piled up the bigger reinforcing particles, consequently impeding plastic deformation, thus increasing the hardness of the composite with the increment of SiC content. Theoretically, it is expected that strengthening effect will take place for the present composite system (10 $\mu$ m Fe reinforced with 75 $\mu$ m SiC). By close reference to the literature, setting the desired weight percentage of the composite samples, and performing related calculations (using equation 1, 2, and 3 as shown in

Appendix C) to characterize the powder in term of volume percentage and expected theoretical density, the results are tabulated as the following.

Table 4.1: Percentage by weight and volume, amount of powders used and theoretical density

| No.      | Quantity | Fe  |            | SiC |            | Volume % |      | Theoretical Density, g/cm <sup>3</sup> |
|----------|----------|-----|------------|-----|------------|----------|------|--|
|          |          | %   | Weight (g) | %   | Weight (g) | Fe       | SiC  |  |
| <b>1</b> | 12       | 100 | 2.00       | 0   | 0.00       | 100.0    | 0.00 | 7.86                                   |
| <b>2</b> | 12       | 95  | 1.90       | 5   | 0.10       | 88.6     | 11.4 | 7.33                                   |
| <b>3</b> | 12       | 90  | 1.80       | 10  | 0.20       | 78.7     | 21.3 | 6.87                                   |
| <b>4</b> | 12       | 85  | 1.70       | 15  | 0.30       | 69.9     | 30.1 | 6.46                                   |

From the table, note that the quantities of samples for all compositions are 12 each. This is because 3 samples of each composition will be sintered at a temperature at a time where there are 4 different temperatures designed for the test starting from 800°C to 1100°C. Thus, the total weight of powders required for the experiment resulted about 89g for Fe powder and 8g for SiC<sub>p</sub>.

## 4.2 Mixing and Compaction

Due to the small volume of the mixtures, the powders are mixed manually using a marble mortar and pestle. This is because the procedure is more relevant and ensures higher homogeneity of mixture than using the actual mixer or blender since powders tends to form agglomerate and stick to the wall of the mixer, thus reducing the volume significantly. The process of compaction is done by using cold press machine; Auto Pelletizer. The mold available produced compacts with 13mm in diameter and have limit of 519MPa for maximum compaction pressure. From literature (Kalpakjian et al., 2006), the suggested suitable compaction pressure for iron powder is about 350MPa to 800MPa.

Since there is no reference that clearly reveals the optimum compaction parameters for the composite, selection of suitable parameters for the research is done by performing several compaction tests. The variables for the test are the load, mass of powders and

dwell time. The pressures are ensured to be in the range suggested by literatures. Results from the initial compaction process tests are as follow:

Table 4.2: Result from compaction by Auto Pelletizer.

| No. | Parameters   | Result  |
|-----|--|---|
| 1   | Powder: 850 $\mu$ m<br>Compaction Pressure: 350MPa<br>Dwell time: 5 min                    |  <ul style="list-style-type: none"> <li>• Not perfectly compacted.</li> <li>• Compact can be easily dissociated.</li> </ul>        |
| 2   | Powder: 850 $\mu$ m<br>Compaction Pressure: 519MPa<br>Dwell time: 30 min                   |  <ul style="list-style-type: none"> <li>• Not perfectly compacted.</li> <li>• Compact can be easily dissociated.</li> </ul>        |
| 3   | Powder: 850 $\mu$ m<br>(reduced mass)<br>Compaction Pressure: 519MPa<br>Dwell time: 30 min |  <ul style="list-style-type: none"> <li>• Not perfectly compacted.</li> <li>• Compact can still be easily dissociated.</li> </ul> |
| 4   | Powder: 10 $\mu$ m<br>Compaction Pressure: 400MPa<br>Dwell time: 5 min                     |  <ul style="list-style-type: none"> <li>• Not perfectly compacted.</li> <li>• Compact can still be dissociated.</li> </ul>       |
| 5   | Powder: 10 $\mu$ m<br>Compaction Pressure: 500MPa<br>Dwell time: 5 min                     |  <ul style="list-style-type: none"> <li>• Perfectly compacted.</li> <li>• Smooth surface.</li> </ul>                             |

The table shows that sample 5 is the best sample to chose. The parameters are suitable for both; the sample and the machine. Sample 1 until sample 3 resulted in defect mainly due to the low pressure applied. The samples with 850 $\mu$ m require higher compaction pressure which cannot be achieved by the Auto Palletizer machine. Other compaction

machines which offer larger compaction pressure are available but the requirement of a huge amount of raw materials is another issue. Limited volume of SiC powder hinders the utilization of machines with large mold. Thus, Fe powder of 850 $\mu$ m in size is taken out from the alternatives. In conclusion, for the compaction stage, the compaction pressure and dwell time is set to 500MPa and 5 minutes respectively. After finalizing the compaction parameters, all 48 samples are compacted. The dimensions and density of the compacts are tabulated in Table I as attached in Appendix D.

From observations, the average values for green densities are about 80% of theoretical value (sample calculations are attached in Appendix B). These high values of green densities which appear as a result of low porosity are the implication of the multi-sizes particles used where  $Fe_p$  is approximately 5 times smaller than  $SiC_p$ . The smaller size of Fe particles filled up the gaps between the larger reinforcement particles, leading to a smaller volume of gaps within the compacts. In addition to that, Lin et al. (2003) verified that under the condition where the reinforcement particle size to the matrix particle exceeds 2, many matrix particles surrounds and piled up reinforcing particles. Moreover, large reinforcing particle also have a large contact area with the matrix, so reinforcing particles can impede the sliding of matrix particles under compressive stress, which is likely to reduce the size of gaps between the particles.

### **4.3 Sintering**

The green compacts were sintered at 800°C, 900°C, 1000°C and 1100°C for 45 minutes in Argon atmosphere to avoid surface contamination. The heating and cooling rates of sintering process were set according to literature; 5°C/min and 10°C/min respectively. The dimensions of the sintered compacts are neglected due to the observation of the undersized difference between the green and sintered compacts which are approximately 0.001%. Thus, the shrinkage ratio is insignificant. Sintered density measured by Archimedes instrument are tabulated and attached in Appendix E. Plots of the experimental data, comparing the green and sintered densities for all sintering temperature and composition of SiC are shown in the next pages for further analysis.

**Green and Sintered Density vs. Amount of SiC  
of Compacts Sintered at 800°C**

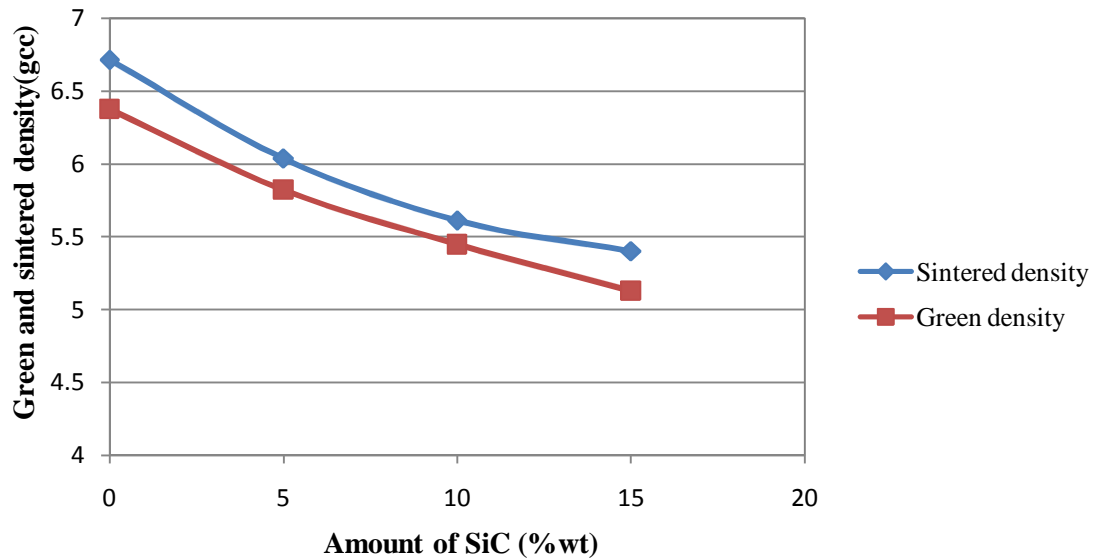


Figure 4.1: Green and sintered density of composites sintered at 800°C.

**Green and Sintered Density vs. Amount of SiC  
of Compacts Sintered at 900°C**

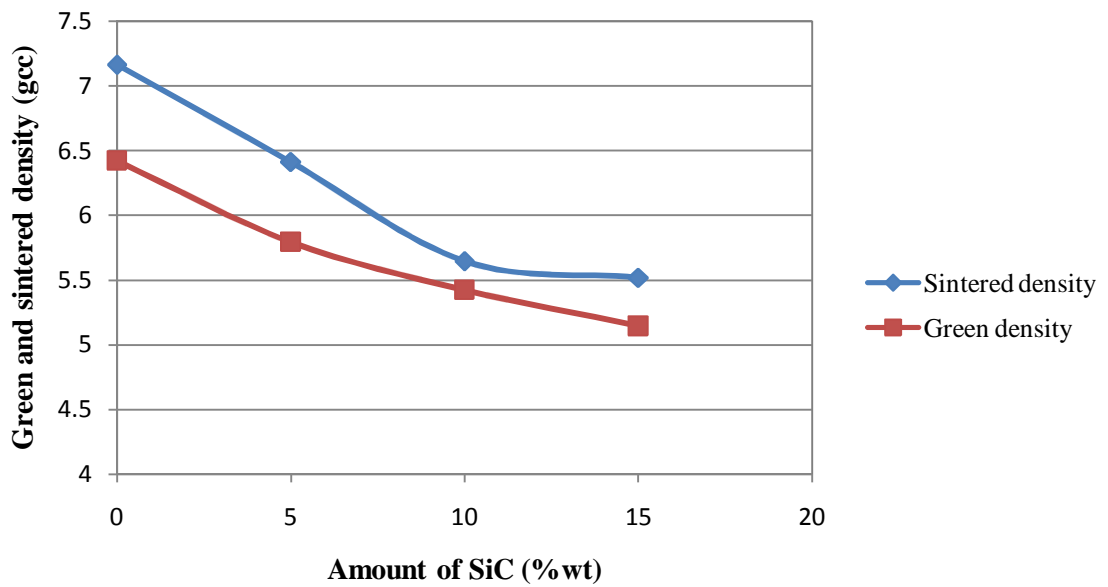


Figure 4.2: Green and sintered density of composites sintered at 900°C.

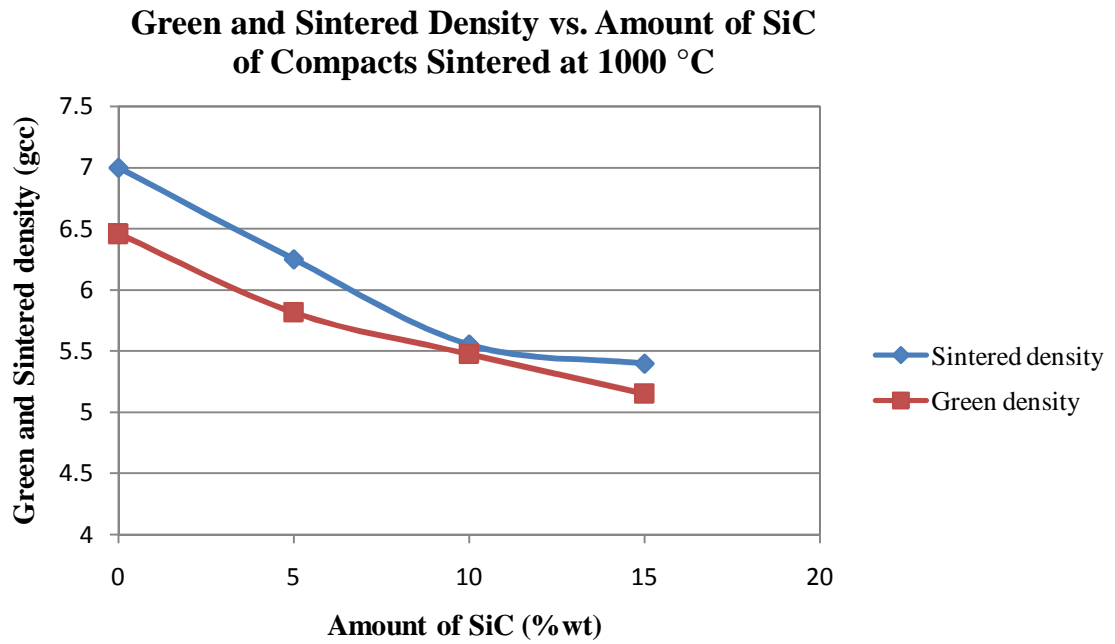


Figure 4.3: Green and sintered density of composites sintered at 1000°C.

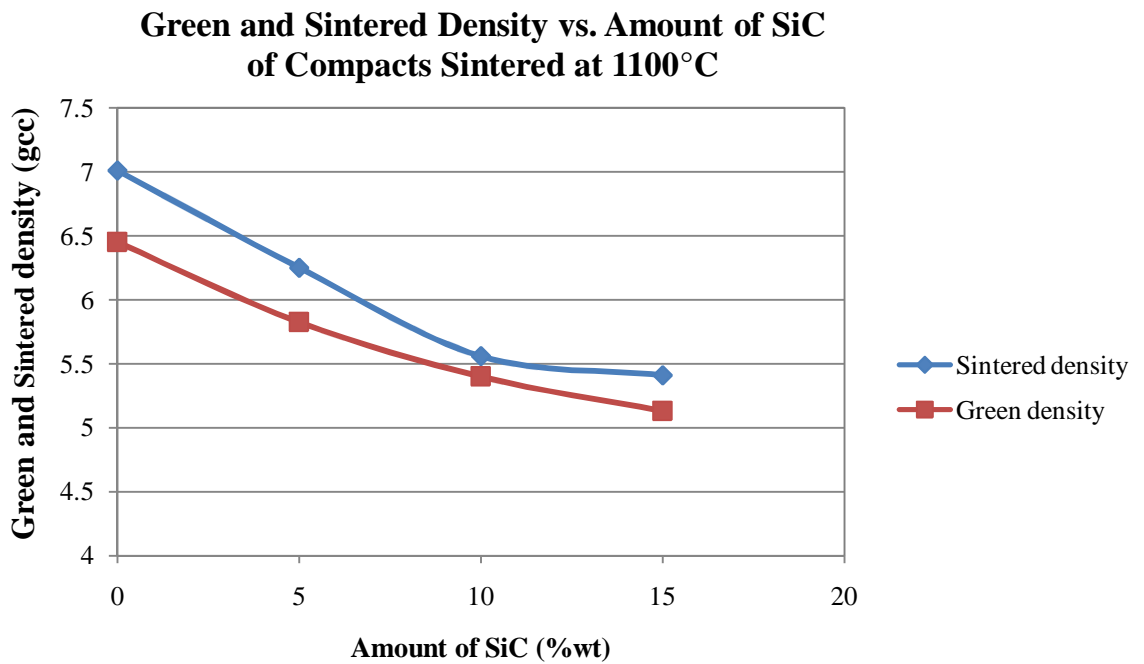


Figure 4.4: Green and sintered density of composites sintered at 1100°C.

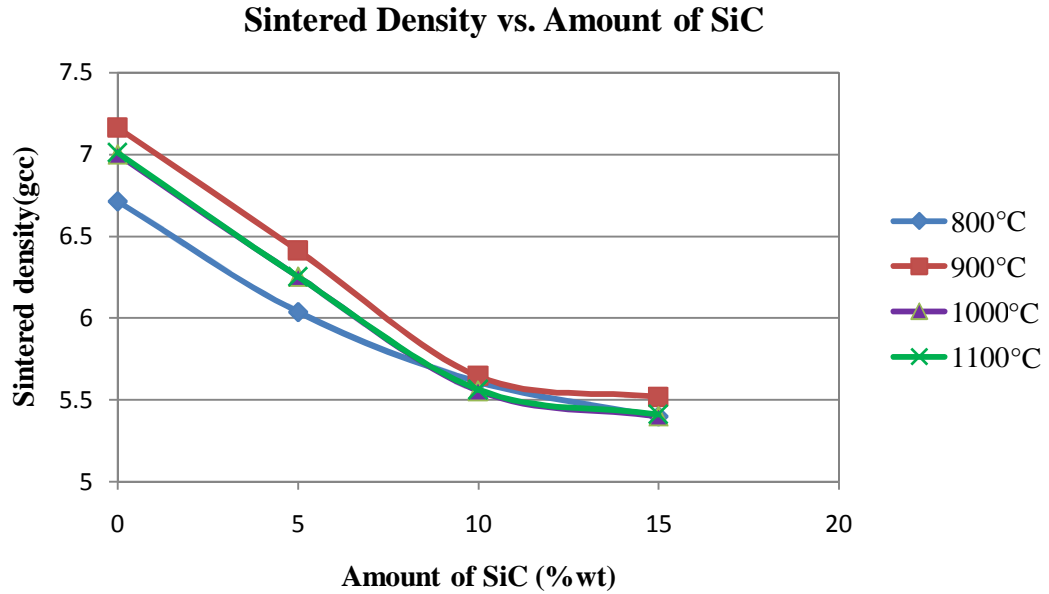


Figure 4.5: Sintered density versus amount of SiC of composites for all sintering temperatures.

It was clearly observed from the figures shown that the presence of SiC<sub>p</sub> reinforcements caused density reduction. The plot shows a trend such that the increment of volume of reinforcing particles reduced the sintered density of the composite. This trend obeyed the rules of mixture which is based on the assumption that “a composite property is the volume weighed average of the matrix and reinforcement properties”, Kopeliovich (2010). Thus, with an increasing volume of reinforcement which possesses lower density than the matrix, the density of the composite is likely to be reduced accordingly. Comparing the green and sintered density, it is clearly shown in the figures that all density increased after sintering and the sintered density increased with increasing sintering temperature due to the improvement of densification at higher temperatures.

In addition, evaluation on the average sintered density versus theoretical density reveals that the composites produced in this research owned about 87% of the theoretical density (sample calculations attached in Appendix C). This result might be due to the earlier step which is the compaction phase. The compaction pressure applied in the experiment is not the highest pressure recommended, thus the green density produced is not having an optimum green properties. The conditions of having non-optimum green

compacts draw in demands for higher sintering temperature or sintering time. Consequently, the sintered density will not achieve its optimum value due to the lacking properties of green compacts.

Apart from that, Figure 4.5 clearly shows that the highest values for sintered densities for all mixtures are obtained at the same sintering temperature which is at 900°C. However, after that temperature, the density drops or remains relatively constant with increasing of temperature. This finding is comparable to result obtained in the experiment conducted by Feng et al. (2007), where they found that density of sintered Fe compacts is lower for sample from 1350°C compared to samples from 1100°C. Whereas, this present study appeared to obtain a lower sintering temperature as an optimum temperature which produced the optimum sintered density. It can be said that the densification degree is higher for samples sintered at 900°C compared to samples sintered at higher temperatures (1000°C and 1100°C).

The results can be analyzed further with reference to the mechanism of plastic deformation. Plastic flow is accelerated at high temperature, which enhances the densification process as indicated by Bingham plastic model. As a result, parts of atomic group in the powders fill into the neighboring pores by plastic flow. However, an expansion of pores called Ostwald ripening might occur at these high sintering temperatures (Randall, 1998). In this case, a certain small pores formed at grain boundaries through vacancy diffusion will deform and even gather together to form big pores because of the effect of plastic deformation. When the sizes of these big pores are greater than a critical size, they will grow and merge each other, and then their irregular shape change into spherical shape which will consequently reduce the density of the samples sintered at high temperature (1000°C and 1100°C).

Besides, according to sintering kinetics as presented by Mrowee (1980), “the higher sintering temperature, the higher the densification degree, but too high a sintering temperature is unfavorable to enhance the densification degree”. This is due to the evolution of pores and decomposition of elements available in the composite mixtures. As proven by Chakthin et al. (2008), the decomposition of SiC particles in the composites resulted in growth of the voids surrounding the reinforcement particles.

They observed that the decomposition of SiC particles was thermally activated at higher sintering temperatures which encourage the growth of voids since the decomposition also initiated the reduction of the SiC particle size.

#### 4.4 Microhardness

Microhardness test was performed using Vickers Test equipment with 300g load at 15s dwell time after the samples have been polished. 5 readings are taken in random area on the samples and the average value is calculated. The results for the test are tabulated in Table III (Appendix F). The simplified table is shown below.

Table 4.3: Summary of micro-Vicker Test for all samples

| T <sub>sinter</sub> (°C) \ wt% SiC | 0      | 5       | 10      | 15      |
|------------------------------------|--------|---------|---------|---------|
| 800                                | 552.98 | 976.56  | 1073.38 | 1157.93 |
| 900                                | 718.72 | 1264.63 | 1390.37 | 1634.42 |
| 1000                               | 844.08 | 1233.12 | 1061.72 | 1322.64 |
| 1100                               | 959.48 | 1246.00 | 1287.90 | 1329.15 |

From the data, it is observed that all Fe-SiC samples are able to provide strengthening as the values of HV obtained are higher than HV of the pure Fe samples. Besides, researches conducted by Bell and Dunford (1980) and Fabregue D. et al. (2010), reveals that HV for sintered pure iron compacts are 220HV and 400HV. With comparison to those literatures, it is safe to say that the data obtained from present hardness tests are valid because they are extremely greater than the previous findings. The significant improvement of hardness might be due to the different ratio of Fe and SiC sizes used; where in this research, SiC particles is larger than Fe, whereas in most of the literatures, Fe is smaller than reinforcement particles. The maximum hardness, 1634.42HV is achieved from the composite reinforced with 15% of SiC particle sintered at 900°C. To further analyze the data, the graphs of hardness value versus the composition of SiC are plotted as shown in the following pages.

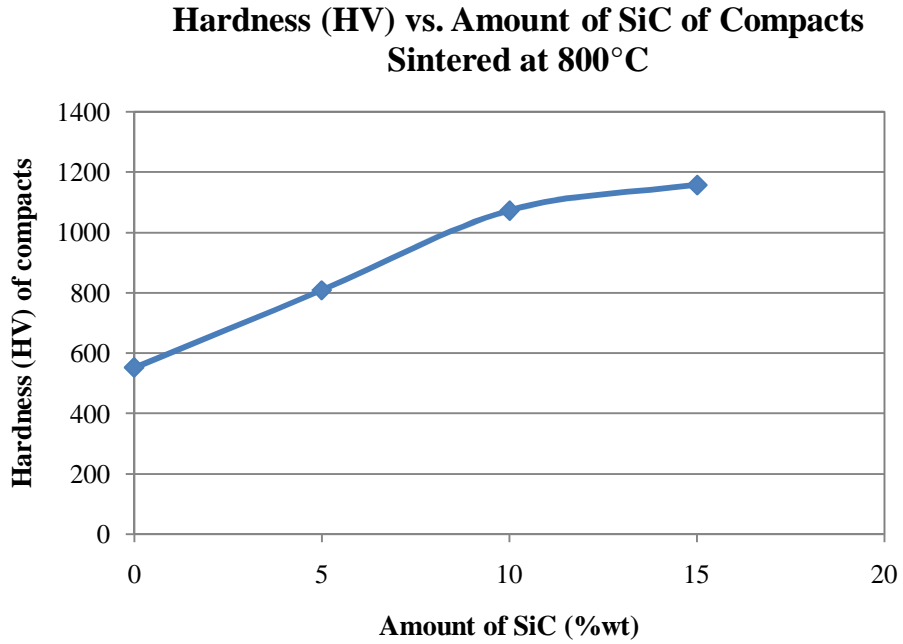


Figure 4.6: Hardness (HV) versus amount of SiC of compacts sintered at 800°C.

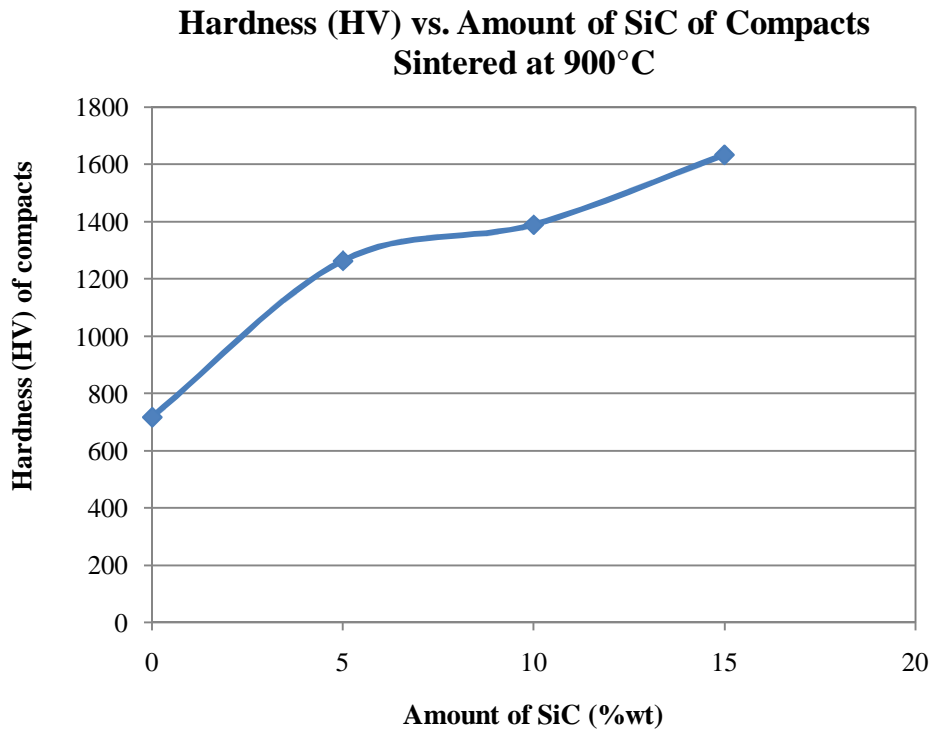


Figure 4.7: Hardness (HV) versus amount of SiC of compacts sintered at 900°C.

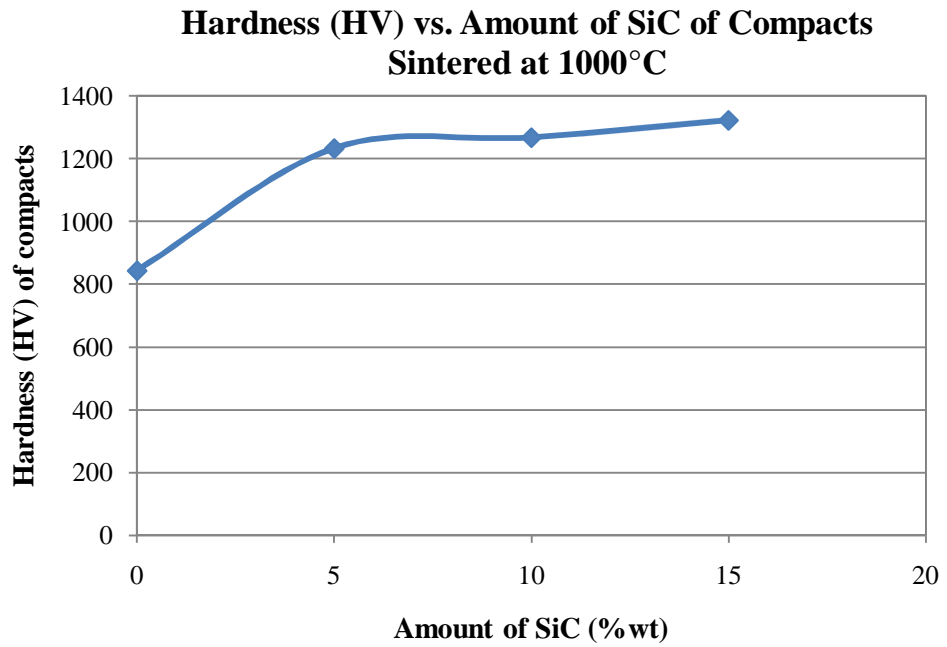


Figure 4.8: Hardness (HV) versus amount of SiC of compacts sintered at 1000°C.

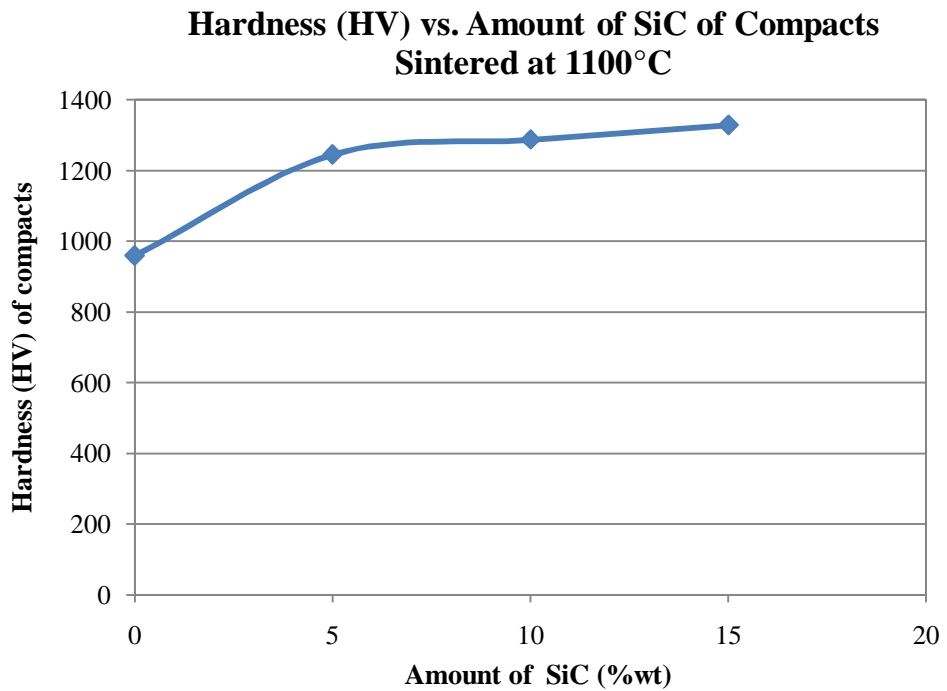


Figure 4.9: Hardness (HV) versus amount of SiC of compacts sintered at 1100°C.

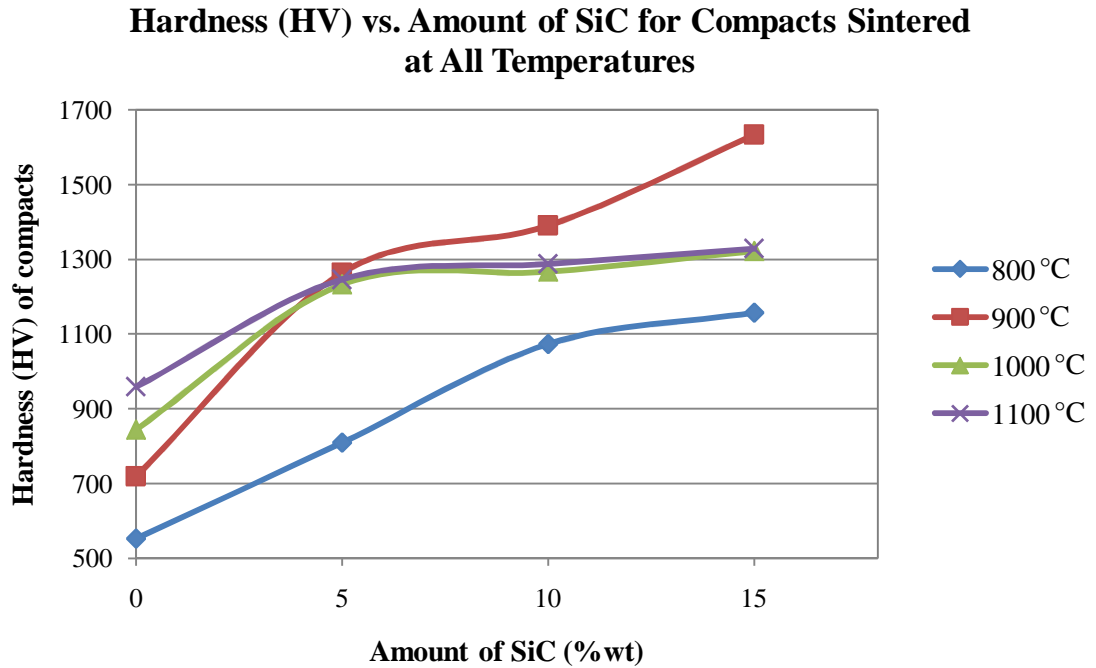


Figure 4.10: Hardness (HV) versus amount of SiC of compacts sintered for all sintering temperatures.

In general, Figure 4.6 to 4.9 show that hardness increased with increasing fraction of reinforcement which complies with most of the cited literatures. Since hardness determines the degree of deformation of materials, the increasing of HV demonstrate that obstruction of plastic deformation occur in the Fe-SiC system. Considering the size of SiC particles which are larger than the matrix, it can effectively obstruct boundary slippage at the interface between Fe particles, causing grain deformation to dominate the plastic deformation. With this mechanism, SiC particles are capable to strengthen Fe-SiC composite when its surface is compressed or indented. Thus, increasing volume of SiC indicates more strongly impeded plastic flow, causing the hardness of Fe-SiC to increase with the amount of reinforcing particle (Lin et al., 2004).

Besides, the decomposition of SiC particles might have took place in the composite, especially at high sintering temperatures. Research conducted by Zhang et al. (2008) on properties of Fe based Cu coated SiC reveals that the coating layer can suppress reaction between Fe and SiC until 1250°C. This statement gives the idea that without

the coating, as in the present study, interface reaction can take place or the decomposition of SiC particles might have thermally activated at temperature lower than 1250°C. During the sintering process, some SiC particles decomposed into Si and C atoms that could diffuse into the Fe particles. Possible reactions are as shown below:



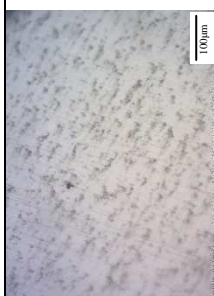
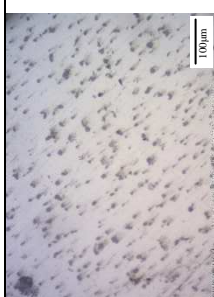
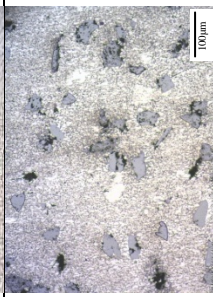
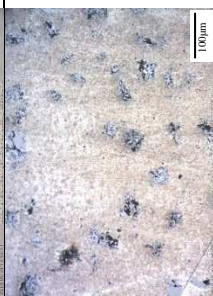
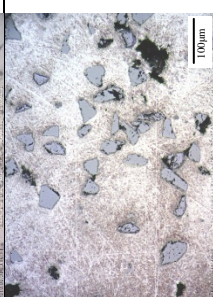
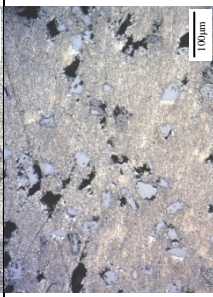
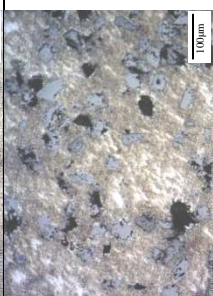
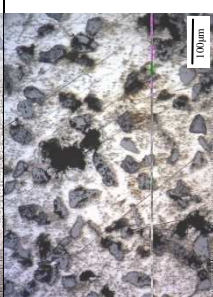
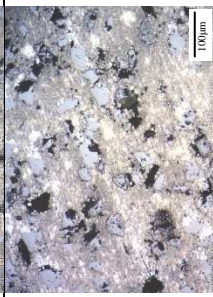
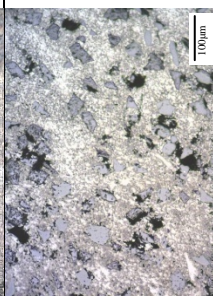
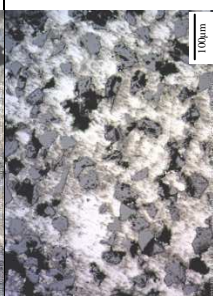
Equation 1 shows the formation of iron-carbon phase in the composite. The development of this phase into ferrite and pearlite structures lead to an effective strengthening mechanism. Iron containing up to 0.51% carbon start solidification with formation of crystals of ferrite at 723°C which then transformed to austenitic phase (Kopeliovich, 2010). During cooling, pearlite which is an alternate layer of ferrite and cementite are formed as the result of decomposition of austenite Fe-C structures. The formation of pearlite phase provides another strengthening mechanism in the Fe-SiC composite (Chakthin et al., 2008). Additionally, both equation 1 and 2 illustrates the possibilities of strengthening by dispersion hardening of Si into the Fe matrix that might also contributed to the increasing hardness of the composite (Libardi et al., 2006).

Meanwhile, Figure 4.10 reveals that the values of HV for compacts sintered at 1000°C and 1100°C are situated in between 800°C and 900°C. In other words, the hardness for composites sintered at 1000°C and 1100°C are lower than hardness of composites sintered at 900°C. The result indicates that the claim about increasing sintering temperature will improve hardness of composite is not typically appropriate for this study. The lower hardness in the composites is most likely attributed to the porosity inside the material (Pagounis et al., 1996). As what have been mentioned in the discussion for sintered density earlier, at higher sintering temperature, the occurrence of Ostwald ripening is possible. A certain small pores formed at grain boundaries through vacancy diffusion can deform and even merge each other. The initially irregular pores become rounded and change size. The expansion of pores reduces the density of the composites which consequently leads to the decrement of hardness.

## 4.5 Microstructure

Microstructural analysis by optical microscopy (50x/0.75 magnification) is performed and the results are as the following:

Table 4.4: Micrographs from optical microscopy for all compacts with various amount of SiC and sintering temperatures.

| Temperature<br>wt% of SiC | 800°C   | 900°C  | 1000°C  | 1100°C  |
|---------------------------|---|--|---|---|
| 0                         |    |    |    |    |
| 5                         |    |    |    |    |
| 10                        |   |   |   |   |
| 15                        |  |  |  |  |

From the image of micrographs, the distribution of elements in the composites can be clearly observed. Analysis made by Chakthin et al. (2008) on the microstructure of sintered Fe-SiC composites is referred to characterize the elements shown in the micrographs. It is agreed that there existed three different microstructural features in the sintered Fe-SiC composites, namely; ferritic iron, lamellar structure of pearlite phase, and porosity as labeled in the figure shown below:

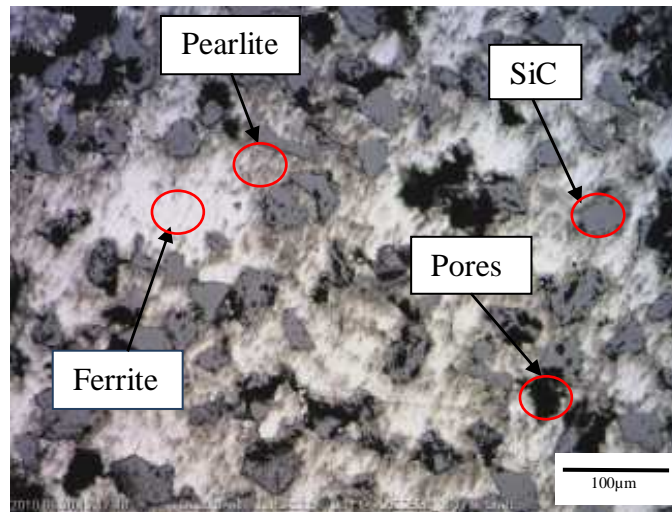


Figure 4.11: Micrograph from optical microscope.

From this information, further observations on the micrographs revealed that SiC particles are uniformly distributed in the composites as the images in Table 4.4 show that the elements dispersed evenly in the compacts. It is found that the size of the particles has decreased from the initial uniform size. This indicates that decomposition of SiC particles has taken place during sintering of the composites. Decomposition of SiC particles resulted in growth of the voids surrounding the particles which can be clearly observed in micrograph for composites with 15% SiC reinforcement sintered at 900°C. The lower part of the image shows the existence of big voids between two decomposed SiC particles.

Besides, the decomposition of SiC particles also lead to the formation of Fe-C phases in the composites which are the ferrite and pearlite structures. The formation of these two structures provided another mechanism of strengthening inside the composites as what have been discussed in the earlier section. It is observed that pearlite zone is lesser in

composites sintered at 1000°C and 1100°C compared to the other two lower temperatures. This condition is most likely due to the retardant of decomposition of the austenite or due to formation of another iron-carbon phase called bainite. As claimed by Herring (2009), pearlite and bainite transformations compete with one another, and the formation of bainite is typified by intermediate hardness and good toughness. This claimed is relevant to this condition, where it is discovered earlier that the hardness of the composites sintered at 1000°C and 1100°C are lower than composites sintered at 900°C which contains more pearlite zones.

Apart from that, it is observed that the size of voids increased with increasing sintering temperatures from 900°C to 1100°C. This is due to expansion behavior of pores where larger pore growing at the expense of smaller pores. At high temperatures, plastic flow is accelerated. This caused a certain small pores which formed at grain boundaries through vacancy diffusion to deform and gather to form big pores because of the effect of plastic deformation as mentioned and discussed thoroughly in section 4.4 earlier.

## CHAPTER 5

### CONCLUSION & RECOMMENDATION

In this research project, powder metallurgy technique was successfully utilized to fabricate Fe-SiC composites. Results obtained are valid and comparable to literatures. Besides, the objectives set up for this research has been accomplished which are basically to produce Fe-SiC composite and to investigate the effect of SiC contents as well as variation of sintering temperatures towards the properties of the composites. The following conclusions have been drawn from this study:

- Fe-SiC<sub>p</sub> composites have been successfully fabricated with fairly uniform distribution of SiC particles.
- Addition of SiC particles improved hardness and offered weight saving to Fe-sintered materials.
- Strengthening mechanisms were provided by impedance of plastic deformation by SiC particles and formation of iron-carbon phases.
- Optimum density and hardness can be obtained at 900°C. Sintered density and hardness increased from 800°C to 900°C. However, higher temperatures caused pore expansion and lowered the densification degree.

Nevertheless, it is recommended for future investigations to examine the elements and phases exist in Fe-SiC composites thoroughly to provide further details on the microstructural behavior and strengthening effects. Besides, it is essential to identify the optimum parameters such as the compaction pressure and most suitable sintering atmosphere to improve the properties of the composites.

## REFERENCES

1. Jennifer S. Franklin 2003, *In-situ Synthesis of Piezoelectric-Reinforced Metal Matrix Composites*, Master of Science Thesis, Virginia Polytechnic Institute and State University, Blacksburg, VA.
2. Ibrahim, Mohamed, and Lavernia, *Particulate reinforced metal matrix composites – A Review*. Journal of Materials Science, 1991. **26**: p. 1137-1156.
3. Lyndon N. Smith 2003, *A Knowledge Based system for Powder Metallurgy Technology*, United Kingdom, Professional Engineering Publishing.
4. S.M. Zebarjad, S.A. Sajjadi, and E.Z. Vahid Karimi, 2008, “Influence of Nanosized Silicon Carbide on Dimensional Stability of Al/SiC Nanocomposite,” *Hindrawi Publishing Corporation, Research Letters in Material Science*, **Vol. 2008**, 1-4.
5. E. Pagounis, M. Talvitie and V.K. Lindroos, 1996, “Influence of the Metal/Ceramic Interface on the Microstructure and Mechanical Properties of HIPed Iron-Based Composites”, *Composites Science and Technology*, *Elsevier Science Limited*, **56**: p. 1329-1337.
6. H. Tanino, K. Ando, S. Omura, T. Miyake, M. Kondoh, and N. Matsumoto, 2008, “Iron-based sintered material and production method thereof,” Retrieved on 17 March 2010: 1806 hrs, from Patentdocs database.
7. Mukherjee, S.K. & Upadhyaya, G.S., 1985, “Mechanical Behavior of Sintered Ferritic Stainless Steel-Al<sub>2</sub>O<sub>3</sub> Particulate Composite Containing Ternary Additions”, *Material Science Engineerin*, **A75**: 67-78.

8. Bryggman, U. & Lindqvist, J.O., 1992, “HIPed Wear Resistant steel-matrix MMCs”, *Non-Ferrous Materials, Metal Powder Industries Federation, Princeton, NJ, Vol. 6*: 185-197.
9. Talvitie, M.J. & Lindroos, V.K., 1994, “Microstructure and Properties of Ceramic Reinforced Super-Duplex Stainless Steel”, *Powder Metallurgy'94 World Congress, Societe Fraincaise de Metallurgie at de MAteriaux, Paris, 30*: 1333-1336.
10. Naresh Prasad, 2006, “Development & Charaterization of MMC using Red Mud an Industrial Waste for Wear Resistant Application”, Doctor of Philosophy Thesis, National Institute of Tech. India.
11. J. Zhang, R.J. Perez, M. N. Gungor and E.J.Lavernia, 1992, “Damping Characteristics of Graphite Particulate Reinforced Aluminium Composites”, *Developments in Ceramics and Metal Matrix Composites. Kamleshwar Upadhya, ed., Warrendale, PA: TMS Publication*, p. 203-217.
12. S. Chakthin, M. Morakotjinda, T. Yodkaew, N. Torsangtum, R. Krataithong, P. Siriphol, O. Coovattanachai, B. Vetayanugul, N. Thavarungkul, N. Poolthong, and R. Tongsri, 2008, “Influence of Carbides on Properties of Sintered Fe-Base Composite”, *Journal of Metals, Materials and Minerals, 18,2*: 67-70.
13. Nikhilesh Chawla and Yu-Li Shen, 2001, “Mechanical Behavior of Particle Reinforced Metal Matrix Composites,” *Advance Engineering Material, Wiley Interscience, 3:6*, 357-370.
14. Y.C. Lin, H.C. Li, S.S. Liou, and M.T. Shie, 2003, “Mechanism of plastic deformation of powder metallurgy metal matrix composite of Cu-Sn/SiC and 6061/SiC under compressive stress,” *Material Science and Engineering, Elsevier B.V., 373*, 363-369.

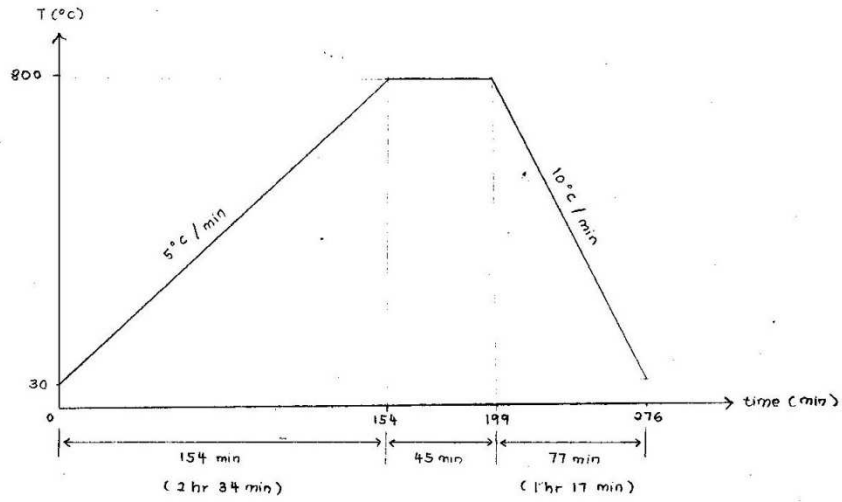
15. X.D. Yu, Y.W. Wang and F.C. Wang, 2007, "Effect of particle size on mechanical properties of SiC<sub>p</sub>/5210 Al metal matrix composite," *Transaction of Nonferrous Metal Society China*, **17**, 276-279.
16. D.L. Zhang, J. Liang and J. Wu, 2004, "Processing of Ti<sub>3</sub>Al-SiC nanocomposites using high energy mechanical milling," *Material Science and Engineering A, Elsevier B.V.*, **375-377**, 911-916.
17. K.T. Kim, J.H. Cho and J.S. Kim, 2000, "Cold Compaction of Composite Powders," *Journal of Engineering Materials and Technology, American Society of Mechanical Engineers*, **122**, 119-128.
18. Serope Kalpakjian & Steven Schmid, 2006, "Processing of Metal Powders" in *Manufacturing Engineering and Technology* (5<sup>th</sup> Edition), Singapore; Pearson Education.
19. K. Feng, Y. Yang, M. Yong, J. Wu, and S. Lan, 2008, "Intensified sintering of iron powders under the action of an electric field: Effect of technologic parameter on sintering densification," *Journal of Material Processing Technology, Elsevier B.V.*, **208**, 264-269.
20. Kopeliovich D., 10 July 2010 (1645 hour), *Estimations of composite materials properties*,  
<[http://www.substech.com/docuwi/estimations\\_of\\_composite\\_materials\\_properties](http://www.substech.com/docuwi/estimations_of_composite_materials_properties)>, Substances and Technologies Article.
21. Mrowee, S., 1980, *Defects and Diffusion in Solids* (1<sup>st</sup> Edition). Elsevier; Amsterdam.
22. T. Bell and N. Dunford, *Powder Metallurgy*, No. 1, 1980, 95. – G.S. Upadhyaya, 2000, "Sintered Fe" in *Sintered Metallic and Ceramics Materials; Preparation, Properties and Applications*, England; John Wiley and Sons.

23. Herring, D. H., (2009), 10 July 2010 (1805 hour), *What Happens to Steel During Heat Treatment?- Part 1 Phase Transformation*, < <http://vacaero.com/News-Info-From-Industrial-Heating-Magazine/News-Info-From-Industrial-Heating-Magazine/What-Happens-to-Steel-During-Heat-Treatment-Part-1-Phase-Transformations.html>>, VAC Aero International Inc.

# APPENDIX A – Details of Sintering Conditions

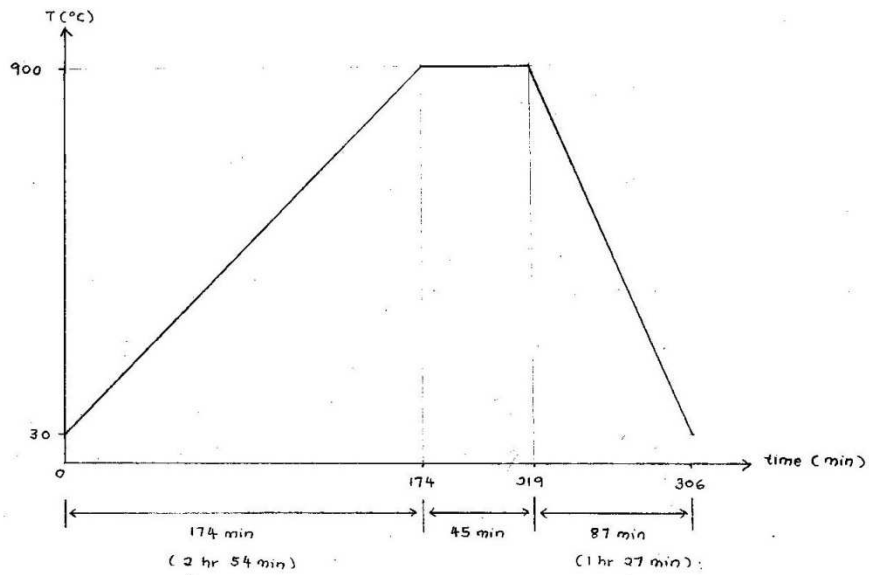
Plots of sintering conditions for 800°C and 900°C

1st batch (dwell @ 800°C) - 20 April 2010



Total : 4 hr 36 min

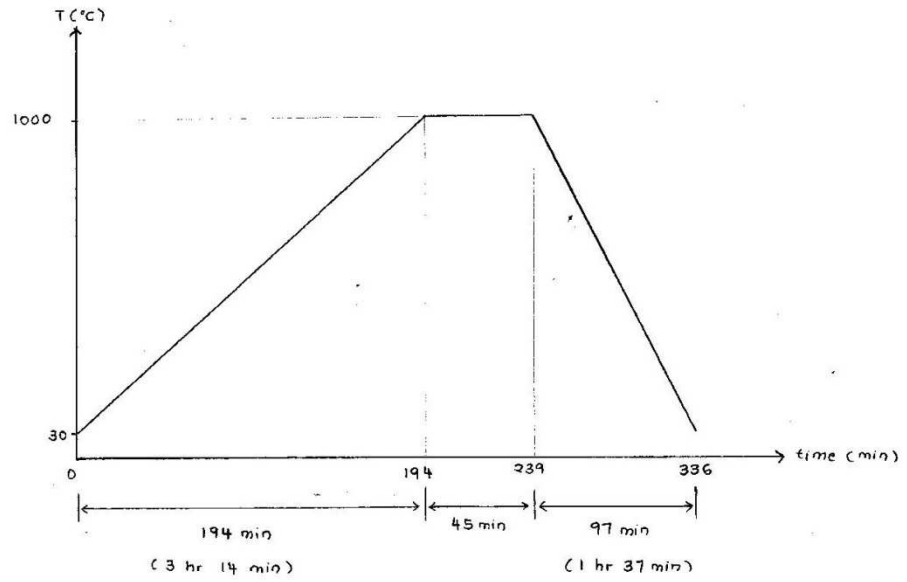
2nd batch (dwell @ 900°C) - 21 April 2010



Total : 5 hr 06 min

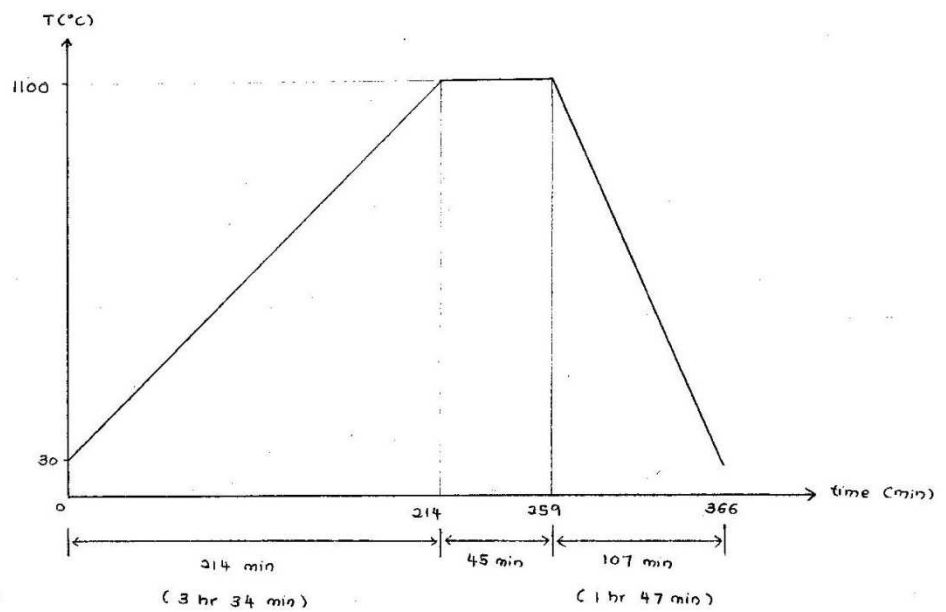
## Plots of sintering conditions for 1000°C and 1100°C

3rd batch (dwell @ 1000°C) - 23 April 2010



Total: 5 hr 36 min

4th batch (dwell @ 1100°C) - 23 April 2010



Total: 6 hr 06 min

## APPENDIX B – Figures of Final Samples

Pictures of the mounted and polished samples



Top view



Orthogonal view



Side view



Mounted and polished samples.

## APPENDIX C – Calculations for Density of Composites

Equations and sample calculations:

1. Weight percentage, % wt

$$f_w = \frac{M_f}{M_f + M_m}$$

Where:  $f_w$  is the weight fraction.

$M_f$  is the mass of ceramic reinforcement.

$M_m$  is the mass of metal matrix.

Then, **%wt =  $f_w \times 100\%$**

e.g.  $f_w = \frac{0.10 \text{ g}}{(0.10 + 1.90)\text{g}}$   
 $= 0.05$   
**%wt =  $0.05 \times 100 = 5\%$**

2. Volume percentage, % vol from % wt

$$f = \frac{V_f}{V_f + V_m}$$

$$f = \frac{\frac{M_f}{\rho_f}}{\frac{M_f}{\rho_f} + \frac{M_m}{\rho_m}}$$

$$f = \frac{\rho_f}{\frac{f_w M}{\rho_f} + \frac{(1-f_w)M}{\rho_m}}$$

$$f = \frac{f_w}{f_w + (1-f_w) \frac{\rho_f}{\rho_m}}$$

Where:  $f$  is the volume fraction.

$\rho_f$  is the density of ceramic reinforcement.

$\rho_m$  is the density of metal matrix.

Then, **%vol = f x 100%**

$$\begin{aligned} \text{e.g. } f &= \frac{(0.05/3.22)}{(0.05/3.22) + (0.95/7.86)} \\ &= 0.1138 \\ \%V_f &= 0.1138 \times 100 = 11.38\% \\ \%V_m &= 100 - 11.38 = 88.62\% \end{aligned}$$

3. Theoretical density,  $\rho_{th}$

$$\rho_{th} = (\rho_w \times \%vol_w) + (\rho_m \times \%vol_m)$$

Where:  $\rho_w$  is the density of ceramic reinforcement.

$\rho_m$  is the density of metal matrix.

$$\begin{aligned} \text{e.g. } \rho_{th} &= (3.22\text{g/cm}^3 \times 0.1138) + (7.86\text{g/cm}^3 \times 0.8862) \\ &= 7.33 \text{ g/cm}^3 \end{aligned}$$

4. Evaluation on green density with theoretical density

$$\% \text{ difference} = \frac{\text{Theoretical density} - \text{Green Density}}{\text{Theoretical density}} \times 100\%$$

e.g. 5% SiC

$$\begin{aligned} \% \text{ difference} &= \frac{7.33 \text{ g/cm}^3 - 5.827 \text{ g/cm}^3}{7.33 \text{ g/cm}^3} \times 100 \\ &= 20.5\% \\ \% \text{ density} &= 100\% - 20.5\% \\ &= 79.5\% \text{ from theoretical density} \end{aligned}$$

5. Evaluation on sintered density with theoretical density

$$\% \text{ difference} = \frac{\text{Theoretical density} - \text{Sintered Density}}{\text{Theoretical density}} \times 100\%$$

e.g. 5% SiC

$$\begin{aligned} \% \text{ difference} &= \frac{6.412 \text{ g/cm}^3 - 7.33 \text{ g/cm}^3}{7.33 \text{ g/cm}^3} \times 100 \\ &= 12.5\% \\ \% \text{ density} &= 100\% - 12.52\% \\ &= 87.5\% \text{ from theoretical density} \end{aligned}$$

## APPENDIX D – Table of Dimensions and Green Density of Compacts

Table I: Dimensions and green density of compacts.

| Label | % SiC | m powder        | T <sub>sinter</sub> (°C) | d (mm) | h (mm) | m compact (g) | v compact (mm <sup>3</sup> ) | ρ green(g/cm <sup>3</sup> ) |
|-------|-------|-----------------|--------------------------|--------|--------|---------------|------------------------------|-----------------------------|
| 1     | 0     | 2 g Fe          | 800                      | 13.04  | 2.32   | 1.962         | 0.310                        | 6.332                       |
| 2     |       |                 |                          | 13.04  | 2.29   | 1.966         | 0.306                        | 6.419                       |
| 3     |       |                 |                          | 13.04  | 2.31   | 1.970         | 0.309                        | 6.377                       |
| 4     |       |                 | 900                      | 13.04  | 2.31   | 1.965         | 0.309                        | 6.370                       |
| 5     |       |                 |                          | 13.04  | 2.29   | 1.973         | 0.306                        | 6.442                       |
| 6     |       |                 |                          | 13.04  | 2.29   | 1.972         | 0.306                        | 6.448                       |
| 7     |       |                 | 1000                     | 13.04  | 2.29   | 1.968         | 0.306                        | 6.426                       |
| 8     |       |                 |                          | 13.04  | 2.29   | 1.984         | 0.306                        | 6.487                       |
| 9     |       |                 |                          | 13.04  | 2.30   | 1.980         | 0.307                        | 6.455                       |
| 10    |       |                 | 1100                     | 13.04  | 2.28   | 1.970         | 0.304                        | 6.470                       |
| 11    |       |                 |                          | 13.04  | 2.28   | 1.959         | 0.304                        | 6.434                       |
| 12    |       |                 |                          | 13.04  | 2.28   | 1.963         | 0.304                        | 6.447                       |
| 16    | 5     | 1.9 Fe + .1 SiC | 800                      | 13.04  | 2.47   | 1.925         | 0.330                        | 5.828                       |
| 17    |       |                 |                          | 13.04  | 2.52   | 1.945         | 0.336                        | 5.787                       |
| 18    |       |                 |                          | 13.04  | 2.56   | 2.000         | 0.341                        | 5.857                       |
| 19    |       |                 | 900                      | 13.04  | 2.47   | 1.907         | 0.330                        | 5.781                       |
| 20    |       |                 |                          | 13.04  | 2.54   | 1.975         | 0.340                        | 5.815                       |
| 21    |       |                 |                          | 13.04  | 2.57   | 1.985         | 0.343                        | 5.791                       |
| 22    |       |                 | 1000                     | 13.04  | 2.52   | 1.975         | 0.337                        | 5.861                       |
| 23    |       |                 |                          | 13.04  | 2.55   | 1.962         | 0.340                        | 5.769                       |
| 24    |       |                 |                          | 13.04  | 2.53   | 1.966         | 0.338                        | 5.819                       |
| 25    |       |                 | 1100                     | 13.04  | 2.47   | 1.915         | 0.330                        | 5.798                       |
| 26    |       |                 |                          | 13.04  | 2.36   | 1.819         | 0.315                        | 5.779                       |
| 27    |       |                 |                          | 13.04  | 2.50   | 1.971         | 0.334                        | 5.903                       |
| 31    | 10    | 1.8 Fe + .2 SiC | 800                      | 13.04  | 2.71   | 1.932         | 0.362                        | 5.338                       |
| 32    |       |                 |                          | 13.04  | 2.65   | 1.955         | 0.353                        | 5.531                       |
| 33    |       |                 |                          | 13.04  | 2.71   | 1.980         | 0.362                        | 5.471                       |
| 34    |       |                 | 900                      | 13.04  | 2.67   | 1.942         | 0.356                        | 5.453                       |
| 35    |       |                 |                          | 13.04  | 2.56   | 1.831         | 0.342                        | 5.356                       |
| 36    |       |                 |                          | 13.04  | 2.72   | 1.983         | 0.363                        | 5.466                       |
| 37    |       |                 | 1000                     | 13.04  | 2.66   | 1.948         | 0.355                        | 5.484                       |
| 38    |       |                 |                          | 13.04  | 2.63   | 1.926         | 0.351                        | 5.483                       |
| 39    |       |                 |                          | 13.04  | 2.66   | 1.943         | 0.356                        | 5.463                       |
| 40    |       |                 | 1100                     | 13.04  | 2.70   | 1.959         | 0.361                        | 5.426                       |
| 41    |       |                 |                          | 13.04  | 2.70   | 1.944         | 0.361                        | 5.385                       |
| 42    |       |                 |                          | 13.04  | 2.61   | 1.881         | 0.349                        | 5.390                       |
| 46    | 15    | 1.7 Fe + .3 SiC | 800                      | 13.04  | 2.88   | 1.962         | 0.385                        | 5.101                       |
| 47    |       |                 |                          | 13.04  | 2.80   | 1.928         | 0.374                        | 5.156                       |
| 48    |       |                 |                          | 13.04  | 2.85   | 1.954         | 0.381                        | 5.134                       |
| 49    |       |                 | 900                      | 13.04  | 2.86   | 1.951         | 0.382                        | 5.108                       |
| 50    |       |                 |                          | 13.04  | 2.84   | 1.950         | 0.379                        | 5.141                       |
| 51    |       |                 |                          | 13.04  | 2.83   | 1.956         | 0.378                        | 5.181                       |
| 52    |       |                 | 1000                     | 13.04  | 2.85   | 1.948         | 0.381                        | 5.112                       |
| 53    |       |                 |                          | 13.04  | 2.84   | 1.963         | 0.380                        | 5.169                       |
| 54    |       |                 |                          | 13.04  | 2.81   | 1.944         | 0.376                        | 5.174                       |
| 55    |       |                 | 1100                     | 13.04  | 2.86   | 1.950         | 0.382                        | 5.105                       |
| 56    |       |                 |                          | 13.04  | 2.82   | 1.948         | 0.377                        | 5.166                       |
| 57    |       |                 |                          | 13.04  | 2.82   | 1.927         | 0.377                        | 5.117                       |

## APPENDIX E – Table of Sintered Density of Compacts

Table II : Sintered density obtained from Archimedes density measuring instrument.

| Label | % SiC | m powder        | T <sub>sinter</sub> (°C) | ρ <sub>green</sub> (g/cm <sup>3</sup> ) | avg (g/cm <sup>3</sup> ) | ρ <sub>sintered</sub> (g/cm <sup>3</sup> ) | avg (g/cm <sup>3</sup> ) |
|-------|-------|-----------------|--------------------------|---|--------------------------|--|--------------------------|
| 1     | 0     | 2 g Fe          | 800                      | 6.332                                   |                          | 6.722                                      |                          |
| 2     |       |                 |                          | 6.419                                   |                          | 6.718                                      |                          |
| 3     |       |                 |                          | 6.377                                   | 6.376                    | 6.702                                      | 6.714                    |
| 4     |       |                 | 900                      | 6.370                                   |                          | 7.029                                      |                          |
| 5     |       |                 |                          | 6.442                                   |                          | 7.205                                      |                          |
| 6     |       |                 |                          | 6.448                                   | 6.420                    | 7.255                                      | 7.163                    |
| 7     |       |                 | 1000                     | 6.426                                   |                          | 6.958                                      |                          |
| 8     |       |                 |                          | 6.487                                   |                          | 7.063                                      |                          |
| 9     |       |                 |                          | 6.455                                   | 6.456                    | 6.976                                      | 6.999                    |
| 10    |       |                 | 1100                     | 6.470                                   |                          | 7.054                                      |                          |
| 11    |       |                 |                          | 6.434                                   |                          | 6.985                                      |                          |
| 12    |       |                 |                          | 6.447                                   | 6.450                    | 6.991                                      | 7.010                    |
| 16    | 5     | 1.9 Fe + .1 SiC | 800                      | 5.828                                   |                          | 5.964                                      |                          |
| 17    |       |                 |                          | 5.787                                   |                          | 6.057                                      |                          |
| 18    |       |                 |                          | 5.857                                   | 5.824                    | 6.09                                       | 6.037                    |
| 19    |       |                 | 900                      | 5.781                                   |                          | 6.259                                      |                          |
| 20    |       |                 |                          | 5.815                                   |                          | 6.335                                      |                          |
| 21    |       |                 |                          | 5.791                                   | 5.796                    | 6.342                                      | 6.412                    |
| 22    |       |                 | 1000                     | 5.861                                   |                          | 6.302                                      |                          |
| 23    |       |                 |                          | 5.769                                   |                          | 6.206                                      |                          |
| 24    |       |                 |                          | 5.819                                   | 5.816                    | 6.243                                      | 6.250                    |
| 25    |       |                 | 1100                     | 5.798                                   |                          | 6.310                                      |                          |
| 26    |       |                 |                          | 5.779                                   |                          | 6.212                                      |                          |
| 27    | 5.903 | 5.827           |                          | 6.235                                   | 6.252                    |  |                          |
| 31    | 10    | 1.8 Fe + .2 SiC | 800                      | 5.338                                   |                          | 5.616                                      |                          |
| 32    |       |                 |                          | 5.531                                   |                          | 5.643                                      |                          |
| 33    |       |                 |                          | 5.471                                   | 5.447                    | 5.574                                      | 5.611                    |
| 34    |       |                 | 900                      | 5.453                                   |                          | 5.665                                      |                          |
| 35    |       |                 |                          | 5.356                                   |                          | 5.542                                      |                          |
| 36    |       |                 |                          | 5.466                                   | 5.425                    | 5.724                                      | 5.644                    |
| 37    |       |                 | 1000                     | 5.484                                   |                          | 5.658                                      |                          |
| 38    |       |                 |                          | 5.483                                   |                          | 5.332                                      |                          |
| 39    |       |                 |                          | 5.463                                   | 5.477                    | 5.670                                      | 5.553                    |
| 40    |       |                 | 1100                     | 5.426                                   |                          | 5.544                                      |                          |
| 41    |       |                 |                          | 5.385                                   |                          | 5.623                                      |                          |
| 42    | 5.390 | 5.400           |                          | 5.517                                   | 5.561                    |  |                          |
| 46    | 15    | 1.7 Fe + .3 SiC | 800                      | 5.101                                   |                          | 5.39                                       |                          |
| 47    |       |                 |                          | 5.156                                   |                          | 5.417                                      |                          |
| 48    |       |                 |                          | 5.134                                   | 5.130                    | 5.316                                      | 5.400                    |
| 49    |       |                 | 900                      | 5.108                                   |                          | 5.831                                      |                          |
| 50    |       |                 |                          | 5.141                                   |                          | 5.538                                      |                          |
| 51    |       |                 |                          | 5.181                                   | 5.144                    | 5.450                                      | 5.516                    |
| 52    |       |                 | 1000                     | 5.112                                   |                          | 5.428                                      |                          |
| 53    |       |                 |                          | 5.169                                   |                          | 5.317                                      |                          |
| 54    |       |                 |                          | 5.174                                   | 5.152                    | 5.448                                      | 5.398                    |
| 55    |       |                 | 1100                     | 5.105                                   |                          | 5.279                                      |                          |
| 56    |       |                 |                          | 5.166                                   |                          | 5.626                                      |                          |
| 57    | 5.117 | 5.129           |                          | 5.413                                   | 5.409                    |  |                          |

## APPENDIX F – Table of Hardness (HV) of Compacts

Table III : HV values measured from Vickers Hardness Test.

| Label | % SiC   | m powder        | T <sub>sinter</sub> (°C) | HV      | HV avg  |
|-------|---------|-----------------|--------------------------|---------|---------|
| 1     | 0       | 2 g Fe          | 800                      | 552.00  |         |
| 2     |         |                 |                          | 555.73  |         |
| 3     |         |                 |                          | 551.21  | 552.98  |
| 4     |         |                 | 900                      | 687.54  |         |
| 5     |         |                 |                          | 699.72  |         |
| 6     |         |                 |                          | 768.90  | 718.72  |
| 7     |         |                 | 1000                     | 888.81  |         |
| 8     |         |                 |                          | 832.65  |         |
| 9     |         |                 |                          | 810.78  | 844.08  |
| 10    |         |                 | 1100                     | 992.34  |         |
| 11    |         |                 |                          | 936.00  |         |
| 12    |         |                 |                          | 950.10  | 959.48  |
| 16    | 5       | 1.9 Fe + .1 SiC | 800                      |         |         |
| 17    |         |                 |                          |         |         |
| 18    |         |                 |                          | 809.42  | 809.42  |
| 19    |         |                 | 900                      | 1215.26 |         |
| 20    |         |                 |                          | 1370.04 |         |
| 21    |         |                 |                          | 1208.58 | 1264.63 |
| 22    |         |                 | 1000                     | 1375.44 |         |
| 23    |         |                 |                          | 1005.10 |         |
| 24    |         |                 |                          | 1318.82 | 1233.12 |
| 25    |         |                 | 1100                     | 1234.88 |         |
| 26    |         |                 |                          | 1170.12 |         |
| 27    | 1333.00 | 1246.00         |                          |         |         |
| 31    | 10      | 1.8 Fe + .2 SiC | 800                      | 1005.67 |         |
| 32    |         |                 |                          | 1213.00 |         |
| 33    |         |                 |                          | 1001.47 | 1073.38 |
| 34    |         |                 | 900                      | 1418.30 |         |
| 35    |         |                 |                          | 1253.10 |         |
| 36    |         |                 |                          | 1499.70 | 1390.37 |
| 37    |         |                 | 1000                     | 1220.50 |         |
| 38    |         |                 |                          | 1313.45 |         |
| 39    |         |                 |                          | 1268.61 | 1267.52 |
| 40    |         |                 | 1100                     | 1386.24 |         |
| 41    |         |                 |                          | 1167.50 |         |
| 42    | 1309.96 | 1287.90         |                          |         |         |
| 46    | 15      | 1.7 Fe + .3 SiC | 800                      | 1150.86 |         |
| 47    |         |                 |                          | 1257.93 |         |
| 48    |         |                 |                          | 1065.00 | 1157.93 |
| 49    |         |                 | 900                      | 1627.83 |         |
| 50    |         |                 |                          | 1659.03 |         |
| 51    |         |                 |                          | 1616.40 | 1634.42 |
| 52    |         |                 | 1000                     | 1422.64 |         |
| 53    |         |                 |                          | 1326.94 |         |
| 54    |         |                 |                          | 1218.34 | 1322.64 |
| 55    |         |                 | 1100                     | 1256.68 |         |
| 56    |         |                 |                          | 1222.57 |         |
| 57    | 1508.20 | 1329.15         |                          |         |         |